June 15, 2016

Dear Editor,

We appreciate the reviewers' suggestions which have considerably improved the manuscript (**acp-2015-939**). Enclosed are point-by-point responses to the reviewers. We hope that with these changes the manuscript will be suitable for publication in "**Atmospheric Chemistry and Physics**"

Thank you very much.

Sincerely,

Seung-Muk Yi

Professor, Dept. of Environmental Health, Graduate School of Public Health

Seoul National University, 1 Gwanak-ro, Gwanak-gu, Seoul 151-742, South Korea

Telephone: (82) 2-880-2736, Fax: (82) 2-762-9105, E-mail: yiseung@snu.ac.kr

Response to Anonymous Referees' Comments

● Journal: ACP

● Title: Characteristics of total gaseous mercury (TGM) concentrations in an industrial complex in southern Korea: Impacts from local sources

● Author(s): Yong-Seok Seo, Seung-Pyo Jeong, Thomas M. Holsen, Young-Ji Han, Eunhwa Choi, Eun Ha Park, Tae Young Kim, Hee-Sang Eum, Dae Gun Park, Eunhye Kim, Soontae Kim, Jeong-Hun Kim, Jaewon Choi, Seung-Muk Yi

● MS No.: acp-2015-939

● MS Type: Research article

● Status: Final Response

● Special Issue: Data collection, analysis and application of speciated atmospheric mercury

Response to Anonymous Referee #1:

General comments

This study analyzed seasonal and diurnal variations of TGM at a sampling site in southern Korea. Sources of TGM affecting the sampling site were investigated by correlating TGM with other pollutants and meteorological data and applying several source-receptor methods utilizing wind direction and back trajectory data. A newer method called the conditional bivariate probability function (CBPF) was used in this study to identify sources of TGM. However, I did not find this method very effective at differentiating between ground and stack emission sources. I find that there are many uncertainties in the CBPF results as well as in the back trajectory results that haven't been addressed in this paper. I have concerns about the methodology (insufficient TGM data, selection of trajectory duration) and interpretation of correlation analysis results. A discussion of how the results vary in the different seasons was also lacking in many places of the paper, even though the results are shown in the figures. Overall, I find that a major revision of this paper is necessary.

Response

Thank you for your comments. We believe we have addressed your concerns in the detailed responses below.

Specific comments

Comment 1

Line 57 – the correlation coefficient of r = -0.08 is very small. It's more accurate to state there is little correlation between TGM and air temperature

Response 1

As suggested, we have rephrased the sentence as follows on Line 56-57.

*"There was a **weak but** statistically significant negative correlation between the TGM concentration and ambient air temperature ($r = -0.08$) ($p < 0.05$)".*

Comment 2

Line 84 – "Atmospheric Hg released from natural and anthropogenic sources leading to

enhanced deposition" Please clarify this statement.

Response 2

As suggested, we have rephrased the sentence as follows on Line 85-92.

"*Atmospheric Hg released from natural and anthropogenic sources when introduced into terrestrial and aquatic ecosystem through wet and dry deposition (Mason and Sheu, 2002) can undergo various physical and chemical transformations before being deposited. Its lifetime in the atmosphere depends on its reactivity and solubility so that depending on its form it can have impacts on local, regional and global scales (Lin and Pehkonen, 1999; Lindberg et al., 2007). A portion of the Hg deposited in terrestrial environments through direct industrial discharge or atmospheric deposition is transported to aquatic system through groundwater and surface water runoff (Miller et al., 2013).***"***

Comment 3

Lines 87-89 – Is this sentence about Hg emissions to the atmosphere and the biogeochemical cycling of Hg or the direct release of Hg from industrial effluent?

Response 3

We mean "the direct release of Hg from industrial effluent. In order to more clarify, we corrected "processes" to "**effluent**" on Line 93-95.

"A previous study also reported that Hg directly released into terrestrial and aquatic ecosystems from industrial ***effluent*** *has influenced surface water, sediment and biological tissue (Flanders et al., 2010)."*

Comment 4

Lines 94 – "coal combustion and waste incinerators" was already mentioned in this sentence.

Response 4

As suggested, we have rephrased the sentence as follows on Line 97-100.

"*…including municipal waste incinerators, medical waste incinerators, electric power generating facilities and cement kilns (Dvonch et al., 1998), ferrous and non-ferrous metal processing, iron and steel manufacturing facilities, and oil and coal combustion (Hoyer et al.,*

1995).”

Comment 5

Line 108 – use “data” instead of “information”

Response 5

As suggested, we corrected “information” to “data” as follows on Line 114.

“…combined with concentration **data** were used to identify…”

Comment 6

Line 138 – What temperature was the heated sampling line maintained at? Why is a heated sampling line necessary for sampling TGM?

Response 6

In this study, the sampling line was heated at about **50 ºC** using heat tape to prevent condensation in gold traps because moisture on gold surface interferes with the amalgamation of Hg.

In order to more clarify, we have rephrased the sentence as follows on Line 142-147.

“*Ambient air at a flow rate of 1.5 L min^{-1} was transported through a 3 m-long heated sampling line (1/4” OD Teflon) in to the analyzer. The sampling line was heated at about **50 ºC** using heat tape to prevent water condensation in the gold traps because moisture on gold surfaces interferes with the amalgamation of Hg (Keeler and Barres, 1999). Particulate matter was removed from the sampling line by a 47 mm Teflon filter.*”

Comment 7

2.3 QA/QC – the measurements were made for a one week period in each season. How often were the manual injections performed? Was there any maintenance activities performed prior to re-deployment of the instrument each time? These are important QA/QC procedures to mention because the instruments were offline for a long period of time.

Response 7

The reviewer is correct. In this study, manual injections were performed prior to every field sampling campaign and we continuously operated Tekran 2537B to measure GEM concentrations in the ambient air.

In order to avoid any confusion, we have rephrased the sentence as follows on Line 159-160.

"*Manual injections were performed prior to every field sampling campaign to evaluate these automated calibrations using a saturated mercury vapor standard.*"

Comment 8

Line 168 – This definition of CPF doesn't seem right because it is not exactly the source contribution. You can replace this sentence with the one in line 177.

Response 8

The reviewer is correct. We have rephrased the sentence as follows on Line 171-173.

"*CPF estimates the probability that the measured concentration will exceed the threshold criterion for a given wind direction.*"

Comment 9

Lines 173-175 – were the wind data measured every 5 min similar to TGM or was it averaged to the nearest hour?

Response 9

In this study, **hourly** meteorological data (air temperature, relative humidity, and wind speed and direction) were obtained from the Automatic Weather Station (AWS) operated by the Korea Meteorological Administration (KMA) (http://www.kma.go.kr).

In order to clarify, we added "hourly" in the sentence as follows on Line 150-152.

"***Hourly*** *meteorological data (air temperature, relative humidity, and wind speed and direction) were obtained from the Automatic Weather Station (AWS) operated by the Korea Meteorological Administration (KMA) (http://www.kma.go.kr) (6 km from the site).*"

This information was also described in Table 2 as follows on Line 533-534.

"***Table 2****. Summary of atmospheric concentrations of TGM and co-pollutants, and meteorological data. Note that TGM was measured every 5-min, and other pollutants and*

meteorological data were measured every 1-hour."

Comment 10

Lines 183-185 –How does this method account for the full distribution of concentrations rather than concentrations exceeding a threshold? Based on Eq. 2, CBPF analyzes the subset of concentrations above a threshold as well. Another thing is how does this method account for sources with different dispersion characteristics? The equation is based on horizontal wind speeds, which is advection rather than dispersion.

Response 10

The statement in question is incorrect since we used a criteria to determine which concentrations to include so we have deleted the sentence.

Comment 11

Lines 193-195 – This explanation is not clear. Can you give some examples of mercury sources with different wind speed dependencies?

Response 11

In order to more clarify, we rephrased the sentence as follows on Line 195-198.

"*The extension to the bivariate case can provide more information on the nature of the sources because different source types such as stack emission sources and ground-level sources can have different wind speed dependencies (prominent at low and high wind speed).*"

Comment 12

Lines 201-215 – this part needs to be rewritten by improving on the wording

Response 12

As suggested, we rephrased the sentence as follows on Line 204-218.

"*The PSCF is a simple method that links residence time in upwind areas with high concentrations through a conditional probability field and was originally developed by Ashbaugh et al. (1985).*

$PSCF_{ij}$ is the conditional probability that an air parcel that passed through the ijth cell had a

high concentration upon arrival at the monitoring site and is defined as the following Eq. (3).

$$PSCF_{ij} = \frac{m_{ij}}{n_{ij}} \quad (3)$$

where, n_{ij} is the number of trajectory segment endpoints that fall into the ij-th cell, and m_{ij} is the number of segment endpoints in the same grid cell (ij-th cell) when the concentrations are higher than a criterion value as measured at the sampling site.

High PSCF values in those grid cells are regarded as possible source locations. Cells including emission sources can be identified with conditional probabilities close to one if trajectories that have crossed the cells efficiently transport the released pollutant to the receptor site. Therefore, the PSCF model provides a tool to map the source potentials of geographical areas."

Comment 13

Line 220 –Please justify the use of 24 hr trajectories. TGM is mainly GEM which has a longer residence time and capable of long range transport. This means a longer trajectory duration would be more suitable.

Response 13

In this study, 24h backward trajectories starting at every hour at a height of 10, 50 and 100 m above ground level were computed using the vertical velocity model because we identified the diurnal variations in TGM concentrations are due to a combination of 1) reactions with an oxidizing atmosphere, 2) changes in ambient temperature and 3) local emissions related to industrial activities. This information was described in Line 422-424.

Previous studies reported that identified the long-range transport of mercury using the ΔTGM/ΔCO enhancement ratio (Choi et al., 2009; Jaffe et al., 2005; Kim et al., 2009; Weiss-Penzias et al., 2003; Weiss-Penzias et al., 2006). The observed ΔTGM/ΔCO was significantly lower than that of Asian long-range transport, but similar to that of local sources in Korea and in US industrial events suggesting that local sources are more important than that of long-range transport in this study. This information was also described in Line 330-346.

Based on the above results, PSCF was performed to identify the local sources over grid cells corresponding to Gyeongsangbuk-do in eastern South Korea.

In addition, we did not find significant differences between TPSCF using 24 h and 48 h backward trajectories (Fig R1).

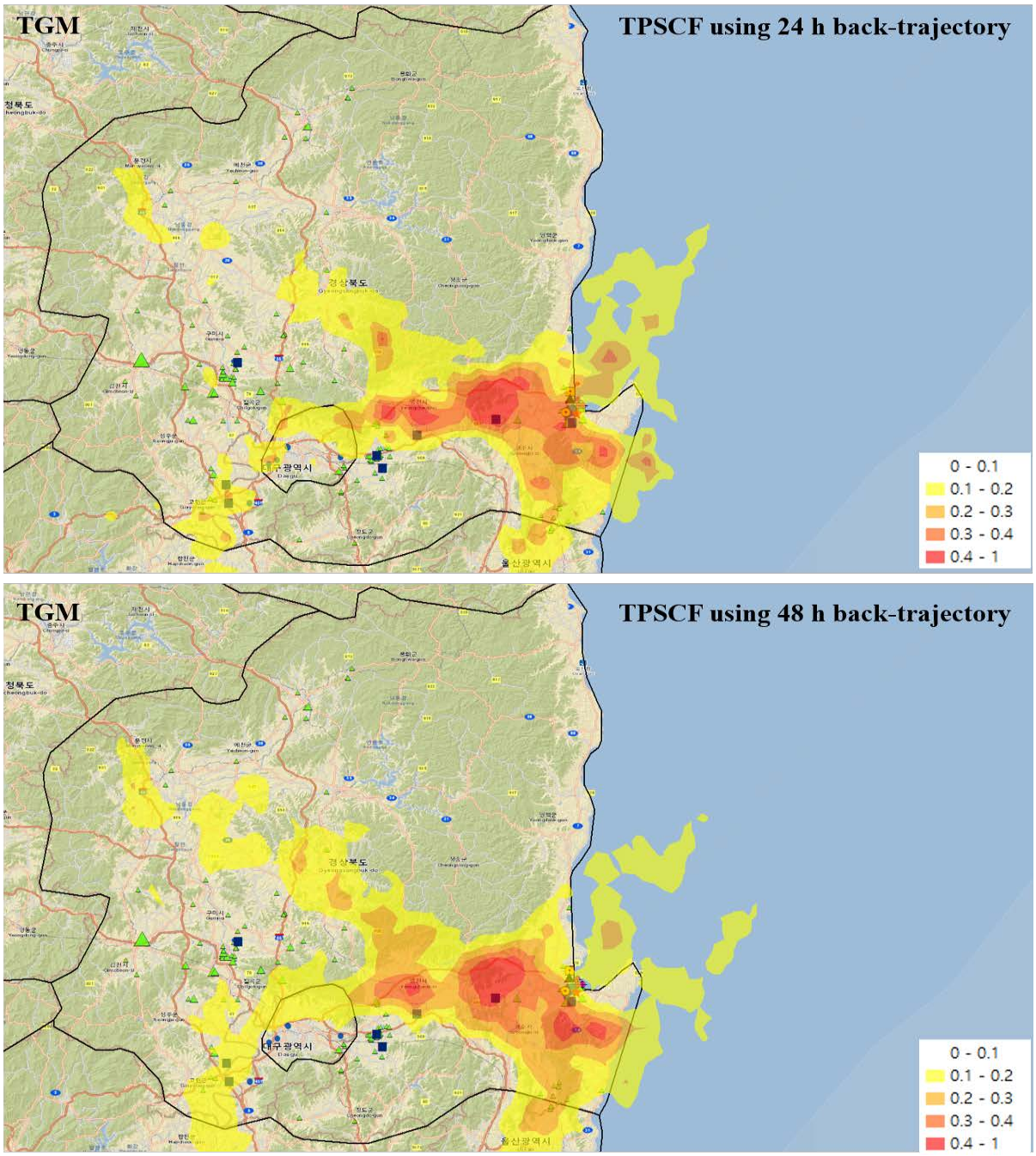

Fig. R1. Comparisons of TPSCF results using 24 h (top) and 48 h (bottom) backward trajectory.

In order to clarify, we have rephrased the sentence as follows on Line 223-227.

"As will be discussed in Section 5.4, 24 h backward trajectories starting at every hour at a height of 10, 50, and 100 m above ground level were computed using the vertical velocity model because local sources are more important than that of long-range transport in this study (It should be noted that PSCF results using 48 h backward trajectories had similar results as the 24 h backward trajectories)."

Comment 14

Line 229 – should be "meteorological data"

Response 14

As suggested, we corrected "meteorology data" to "**meteorological data**" as follows on Line 235.

*"PSCF was calculated with 9 km **meteorological data**"*

Comment 15

Lines 293-294 – This point was not discussed in later sections

Response 15

We have deleted the phrase "*As will be discussed later*" and rephrased as follows on Line 306-308.

"The high TGM concentrations in fall was due to different wind direction (see Fig. S2), sources, relationships with other pollutants and meteorological conditions. More detailed information can be found in Section 5.5."

Comment 16

Lines 299-302 – It should be stated more clearly that combustion was not a source of TGM because of a lack of correlation between TGM and the other combustion pollutant markers.

Response 16

As suggested, we have rephrased the sentence as follows on Line 313-315.

"However, the TGM concentration was not significantly correlated with NO2, CO or SO2 concentrations, suggesting that combustion associated with space heating was not a significant source of TGM (Choi et al., 2009)"

Comment 17

Lines 315 – Fig. S4 shows the CPF and CBPF plots in each season. Should this be discussed in section 5.5? It's not clear how these plots relate to the correlation results.

Response 17

In Section 5.3, we investigated the correlation between TGM and CO and found that local sources are more important than that of long-range transport by the observed ΔTGM/ΔCO. In order to avoid confusion, we have deleted Fig. S4 and rephrased the sentence as follows on Line 326 to Line 329.

"On the other hand, there were no statistically significant correlations between TGM and CO in spring (r = 0.02) (p = 0.78), in summer (r = 0.13) (p = 0.08), or in fall (r = -0.03) (p = 0.69), indicating that TGM and CO were affected by different anthropogenic emission sources in these seasons."

Comment 18

Lines 326-333 – It's surprising that long-range transport from China did not impact this site considering that it affected elevated Hg events in Seoul, Japan, and North America in previous studies. I would think long-range transport impacts a larger region including this sampling location. The TGM/CO slopes during elevated Hg events in Seoul were attributed to both long-range transport and local source impacts (Choi et al., 2009). Is it possible that the one-week sampling period in each season did not capture the long-range transport events? More data is needed to confirm these results. There are also uncertainties from the potential mixing between long-range transported airflows and local air making it difficult to distinguish between distant and local source impacts.

Response 18

We agree with the reviewer's comment. We also think it is possible that the one-week sampling period in each season did not capture the long-range transport events, and more data are needed to confirm these results. Based on the previous studies (Kim et al., 2009; Choi et al., 2009), we analyzed the TGM data in an attempt to identify both long-range transport and local sources of

TGM. Unfortunately, we did not find high concentration events which were defined as at least a 10 h period with hourly average TGM and CO concentrations higher than the average monthly TGM and CO concentrations and high values of TGM/CO ratio (ΔTGM/ΔCO) (0.0052-0.0158 ng m^{-3} ppb^{-1}) and high correlations (r^2>0.5) in this study. Therefore, the observed ΔTGM/ΔCO suggested that local sources are more important than that of long-range transport in this study. However, we believe more can be learned using the larger dataset than just using the one-week sampling period.

In order to any confusion, we added a following sentence on Line 347 to Line 351.

"There are also uncertainties from the potential mixing between Hg associated with long-range transported airflows and local air making it difficult to distinguish between distant and local source impacts. However, it is possible that the one-week sampling period in each season did not capture the long-range transport events, and more can be learned using a larger dataset than just using the one-week sampling period to confirm these results."

Comment 19

Lines 345-346 – what are the time periods for daytime and nighttime concentrations? This sentence states daytime TGM were higher during daytime than nighttime. But in the previous sentence, the minimum TGM concentration occurs in the afternoon.

Response 19

As suggested, we added the time periods for daytime and nighttime as follows on Line 355-356.

"TGM, O_3, CO, SO_2, and temperature in the daytime ***(06:00-18:00)*** *were statistically significantly higher than those in the nighttime* ***(18:00-06:00)*** *($p < 0.05$) except PM_{10} ($p = 0.09$)…"*

In this study, the daytime TGM concentration (5.3 ± 4.7 ng m^{-3}) was statistically significantly higher than that in nighttime (4.7 ± 4.7 ng m^{-3}) ($p < 0.01$). In order to avoid any confusion, we corrected "maximum" to "**increase**" and "minimum" to "**decrease**" as follows on Line 359 to Line 360.

*"TGM generally showed a consistent diurnal variation with an **increase** in the early morning (06:00-09:00) and a **decrease** in the afternoon (14:00-17:00), similar to…"*

Comment 20

Lines 353-355 – You discussed about the land-sea/lake breeze effect on TGM diel patterns from another study in the previous sentence. Does this atmospheric process affect this particular site since it is near the ocean and lower TGM were also observed during daytime?

Response 20

It is possible that the land-sea breeze might affect diurnal variations in TGM concentrations since the sampling site was near the ocean and lower TGM concentrations were observed during the daytime in this study. However, there are several known Hg sources such as iron and steel manufacturing facilities including electric and sintering furnaces using coking around the sampling site.

Although the daytime temperature (14.7 ± 10.0 ºC) was statistically significantly higher than that in the nighttime (13.0 ± 9.8 ºC) ($p < 0.05$), the daytime TGM concentration (5.3 ± 4.7 ng m^{-3}) was statistically significantly higher than those in the nighttime (4.7 ± 4.7 ng m^{-3}) ($p < 0.01$). This is possibly due to a combination of 1) reactions with an oxidizing atmosphere, 2) changes in ambient temperature and 3) local emissions related to industrial activities. To supplement these conclusions CPF and CBPF were used to identify source directions and TPSCF was used to identify potential source locations in "Section *5.6 CPF, CBPF and TPSCF results of TGM"*.

In order to clarify, we rephrased the sentence as follows on Line 376 to Line 384.

"Although it is possible that the land-sea breeze may affect diurnal variations in TGM concentrations since the sampling site was near the ocean and lower TGM were also observed

during the daytime, the higher concentrations in the daytime than those in nighttime were due to local emission sources because the daytime temperature (14.7 ± 10.0 ºC) was statistically significantly higher than that in the nighttime (13.0 ± 9.8 ºC) (t-test, $p < 0.05$) and there was a weak but statistically significant negative correlation between TGM concentration and ambient air temperature ($r = -0.08$) ($p < 0.05$). In addition, there are several known Hg sources such as iron and steel manufacturing facilities including electric and sintering furnaces using coking between the sampling site and the ocean."

Comment 21

Lines 355-356 – The negative correlation between TGM and temperature is very small (as mentioned in the abstract, r = -0.08) despite a significant p-value. It's more accurate to state there is little relationship between TGM and air temperature.

Response 21

As suggested, we have rephrased the sentence as follows on Line 380-382.

"… and there was a weak but statistically significant negative correlation between the TGM concentration and ambient air temperature ($r = -0.08$) ($p < 0.05$)".

Comment 22

Lines 357-360 – Similar to the above comment, the correlation between TGM and O3 is too small (r = -0.18) to suggest that it is indicative of GEM oxidation. It's more correct to state there is little relationship between TGM and O3. If GEM oxidation occurred, GOM concentrations would increase. There are some uncertainties on the net effect on TGM (GEM+GOM).

Response 22

As suggested, we have rephrased the sentence as follows on Line 385-393.

"…there was a weak but negative relationship between the TGM concentrations and O3 concentrations ($r = -0.18$) ($p < 0.01$), suggesting that oxidation of GEM in the oxidizing atmosphere during periods of strong atmospheric mixing was partially responsible for the diurnal variations of TGM concentrations. In addition, oxidation of GEM by bromine species

in the coastal area (Obrist et al., 2011) or by chloride radicals in marine boundary layer (Laurier et al., 2003) might play a significant role. If oxidation of GEM occurred, GOM concentrations would increase. However there are uncertainties on the net effects on TGM (the sum of the GEM and the GOM) since we did not measure GOM concentrations."

Comment 23

Lines 369-378 – The results here are inconsistent. If the small negative correlation between TGM and temperature indicates an increase in mixing height which leads to a decrease in TGM, how can it explain surface emissions in the morning which should increase with temperature? Is there a positive correlation between TGM and temperature in the morning?

Response 23

As suggested, we analyzed a relationship between TGM and temperature in the morning (06:00-09:00) and found that there is a positive correlation between TGM and ambient air temperature. In order to clarify, we added a following sentence on Line 408-412.

"Nonparametric correlations revealed that there is a positive correlation between TGM and ambient air temperature (r_s = 0.11, p=0.27) between 06:00-09:00. The TGM concentration was negatively correlated with O_3 (r_s = -0.33, p<0.01) but positively correlated with NO_2 (r_s = 0.21, p<0.05), suggesting that the increased traffic is the main source of TGM during these time periods."

Comment 24

Section 5.4 – This section is lacking discussion on seasonal differences in the diurnal variation. The fall diurnal pattern appears very different from those in other seasons in Fig. 3. Can you discuss why the TGM were much higher overnight in the fall but daytime concentrations were similar to those in other seasons? Why was there a large drop in TGM from 4:00 to 5:00 in the fall?

Response 24

As suggested, we described more detailed information on Line 413-421 as follows.

"Compared to other seasons, significantly different diurnal variations of TGM were observed

in fall. The daytime TGM concentrations in fall were similar to those in other seasons, however, the nighttime TGM concentrations in fall were much higher than other seasons. As described earlier in Section 5.3, the high TGM concentrations in fall was possibly due to the relationship between other pollutants and meteorological conditions as well as different wind direction and sources. The nighttime TGM concentrations in fall were simultaneously positively correlated with PM_{10} ($r=0.26$) ($p<0.05$) and CO ($r=0.21$) ($p<0.05$) concentrations and wind speed ($r=0.35$) ($p<0.01$), suggesting that the combustion process is an important source during this period."

We could not identify the reason why there was a large drop in TGM from 4:00 to 5:00 in the fall because there were a limited amount of data. However, we believe more can be learned using a larger dataset.

Comment 25

Lines 381-383 – These conclusions are not well-supported by the correlation analyses because the correlation coefficients were very small.

Response 25

As suggested, we rephrased the "Section 5.5 *Diurnal variations"* on Line 353-426.

Comment 26

Line 390 – What are the potential Hg sources from the northeast direction?

Response 26

The potential Hg sources from the northeast direction is due to lots of domestic passenger ships routes. In response to this comment, we have rephrased the sentence as follows on Line 469-471.

"The northeast direction including the East Sea was also identified as potential source areas likely because this is an area with lots of domestic passenger ships routes."

Comment 27

Lines 391-393 – Please clarify this sentence. Are the higher wind speeds associated with stack emissions and lower wind speeds associated with surface emissions? There are several issues or uncertainties with this point. (1) Wind speeds were only measured at one height. How can you tell that the lower wind speeds are from lower elevation and vice-versa? What is the height of the wind measurements? (2) As mentioned in the diurnal variation section, boundary layer mixing occurs during the day. Is it possible to distinguish between ground emissions and stack emissions? (3) It seems only the west directions had both high and low wind speeds, while the east directions had only lower wind speeds (Fig. S1). Thus, CBPF doesn't seem useful when there is a lack of wind speed variation. It appears that it is by coincidence that both ground level and stack emissions were identified in the west direction because there happened to be a wind speed variation from this direction. Based on these points, the CBPF results don't seem to reveal more about TGM sources than CPF. More discussion is needed on the relationship between specific sources and wind speeds. Instead of wind speed, what other variables would be useful for source identification using CBPF?

Response 27

In this study, hourly meteorological data (air temperature, relative humidity, and wind speed and direction) were obtained from the Automatic Weather Station (AWS) operated by the Korea Meteorological Administration (KMA) (http://www.kma.go.kr). This information was described on Line 150-152. We used the wind data measured at a reference height of 10 m.

Although there is a lack of wind speed variation, we found that the CBPF revealed more about TGM sources than CPF (Fig. S6).

The third variable plotted on the radial axis does not need to be wind speed. A previous study reported that temperature can be a useful radial variable (Carslaw, D.C., Beevers, S.D., 2013. Characterising and understanding emission sources using bivariate polar plots and k-means clustering. Environ. Model. Softw. 40 (0), 325-329).

In order to response to this comment, we rephrased the sentence on Line 195-198 and Line 433-450 as follows.

< Line 195-198>

"The extension to the bivariate case can provide more information on the nature of the sources because different source types such as stack emission sources and ground-level sources can have different wind speed dependencies (prominent at low and high wind speed)."

< Line 433-450>

"CBPF shows that the high probabilities from the west occurred under high wind speed (> 3 m s^{-1}) indicative of emissions from stacks as well as low wind speed (≤3 m s^{-1}) indicative of non-buoyant ground level sources (Uria-Tellaetxe and Carslaw, 2014)"

As described in Section 5.4, correlations between TGM and CO revealed that TGM and CO were affected by similar anthropogenic emission sources in winter but affected by different sources in spring, summer and fall, which is supported by Fig. S6 which shows significantly different seasonal patterns of CPF and CBPF for TGM concentrations.

It is difficult to discuss about the different seasonal patterns of CPF and CBPF for TGM concentrations since there were no correlations between TGM and other pollutants in spring, summer and fall. However, compared to Fig. 4, the CPF and CBPF patterns in fall were similar to those during the whole sampling periods. Especially, the nighttime TGM concentration in fall was simultaneously positively correlated with PM10 ($r=0.26$) ($p<0.05$) and CO ($r=0.21$) ($p<0.05$) concentrations and wind speed ($r=0.35$) ($p<0.01$), indicating that the combustion process from the west is an important source during this period.

Since TGM showed a significant correlation with CO ($r=0.25$) ($p<0.05$) and showed a weak positive correlation with PM10 ($r=0.08$) ($p=0.33$) in winter, the combustion source from the west is partially responsible for this result with high wind speed."

Comment 28

Lines 394-395 – Are there industrial sources south of the sampling site? High probability areas are also identified in this direction in the TPSCF plot in Fig. 4.

Response 28

There is Ulsan Metropolitan City located to the south from the sampling site. Ulsan is South Korea's seventh largest metropolis with a population of over 1.1 million and it has more than 700 small and large industrial facilities including petrochemical plants, oil refineries, vehicle and ship factories, and other chemical plants.

In response to this comment, we have added a following sentence on Line 471 to Line 474.

"The south from the sampling was also identified as a likely source area of TGM where Ulsan Metropolitan City, South Korea's seventh largest metropolis with a population of over 1.1 million is located. It includes a large petrochemical complex known as a TGM source (Jen et al., 2013)."

Comment 29

Fig. 4 – the source areas seem confined to the industrial complex near the sampling site because of the short trajectory duration (24 hrs). Use of longer trajectories would help expand the source region and identify potential regional transport to the site. In addition to this uncertainty, other PSCF uncertainties should be discussed.

Response 29

As mentioned earlier in **Response 13**, local sources are more important than that of long-range transport in this study. Therefore PSCF was performed to identify the local sources over grid cells corresponding to Gyeongsangbuk-do in eastern South Korea.

In addition, we did not find significant differences between PSCF using 24 h and 48 h backward trajectories (Fig. R1 in **Response 13**).

In addition, previous studies suggest that **there are increasing uncertainties as backward trajectory distances increase** (Stohl, et al., 2002) and that PSCF modeling is prone to the trailing effect is which locations upwind of sources are also identified as potential sources (Han, et al., 2004a). An alternative to back trajectory calculations in the interpretation of atmospheric trace substance measurements (Stohl, et al., 2002) although this technique does not provide much information on source locations.

Comment 30

Section 5.5 – This section is lacking discussion on the CPF and CBPF results in different seasons. The seasonal plots are shown in Fig. S4, but they are not discussed in this section.

Response 30

In order to response to this comment, we added the sentence as follows on Line 437-450.

"As described in Section 5.4, correlations between TGM and CO revealed that TGM and CO were affected by similar anthropogenic emission sources in winter but affected by different sources in spring, summer and fall, which is supported by Fig. S6 which shows significantly different seasonal patterns of CPF and CBPF for TGM concentrations.

It is difficult to discuss about the different seasonal patterns of CPF and CBPF for TGM concentrations since there were no correlations between TGM and other pollutants in spring, summer and fall. However, compared to Fig. 4, the CPF and CBPF patterns in fall were similar to those during the whole sampling periods. Especially, the nighttime TGM concentration in fall was simultaneously positively correlated with PM10 ($r=0.26$) ($p<0.05$) and CO ($r=0.21$) ($p<0.05$) concentrations and wind speed ($r=0.35$) ($p<0.01$), indicating that the combustion process from the west is an important source during this period.

Since TGM showed a significant correlation with CO ($r=0.25$) ($p<0.05$) and showed a weak positive correlation with PM10 ($r=0.08$) ($p=0.33$) in winter, the combustion source from the west is partially responsible for this result with high wind speed."

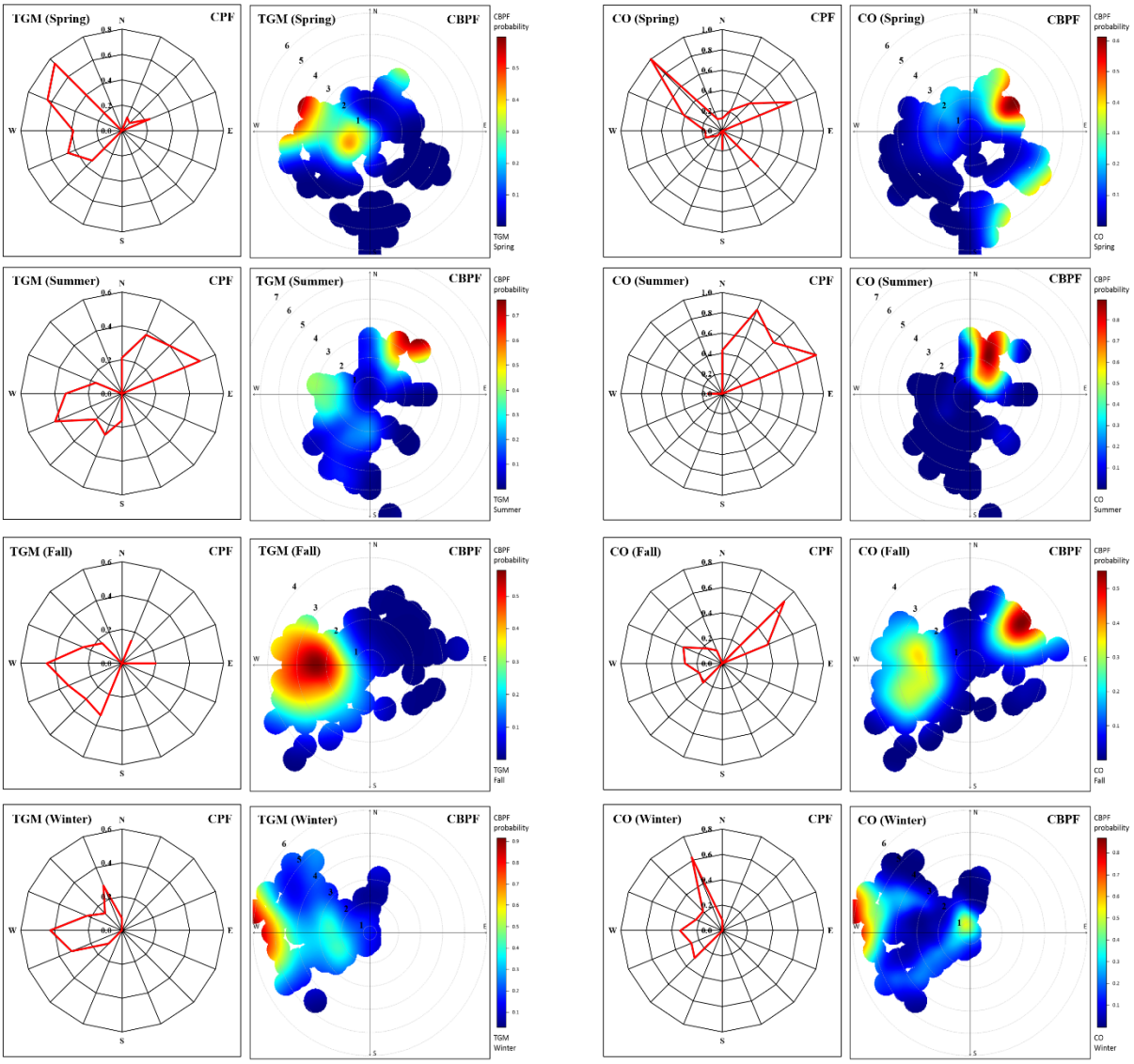

Fig. S6. Comparisons of CPF and CBPF plots for TGM and CO higher than average concentration. The radial axes of CPF and CBPF are the probability and the wind speed (m s^{-1}), respectively.

Comment 31

Lines 421-423 – This conclusion was not discussed in the results section. The wind direction frequency plots in different seasons are shown in Fig. S1 but the results were not discussed in the paper.

Response 31

As suggested, we rephrased the sentence on Line 413-421 as follows.

Comment 32

Lines 427-430 – p-value was significant but the correlation coefficient (magnitude of the relationship) is too small. I also don't understand the logic in these results. There should be a positive TGM and temperature correlation if daytime TGM concentrations were related to surface emissions.

Response 32

In response to this comment, we have rephrased the sentence on Line 363-371 and Line 376-384 as follows.

< Line 363-371>

"The daytime TGM concentration (5.3 ± 4.7 ng m^{-3}) was higher than that in nighttime (4.7 ± 4.7 ng m^{-3}) ($p < 0.01$), which was similar to several previous studies (Cheng et al., 2014; Gabriel et al., 2005; Nakagawa, 1995; Stamenkovic et al., 2007) but different than other study (Lee et al., 1998). Previous studies reported that this is due to local sources which is close to the sampling site (Cheng et al., 2014; Gabriel et al., 2005), positive correlation between TGM concentration and ambient air temperature (Nakagawa, 1995) and increased traffic (Stamenkovic et al., 2007). However, other study suggested that the higher TGM concentration than that in daytime was due to the shallow boundary layer in nighttime, resulting in concentrating the TGM near the surface (Lee et al., 1998)."

< Line 376-384>

"*Although it is possible that the land-sea breeze may affect diurnal variations in TGM concentrations since the sampling site was near the ocean and lower TGM were also observed during the daytime, the higher concentrations in the daytime than those in nighttime were due to local emission sources because the daytime temperature (14.7 ± 10.0 ºC) was statistically significantly higher than that in the nighttime (13.0 ± 9.8 ºC) (t-test, $p < 0.05$) and there was a weak but statistically significant negative correlation between TGM concentration and ambient air temperature ($r = -0.08$) ($p < 0.05$). In addition, there are several known Hg sources such as iron and steel manufacturing facilities including electric and sintering furnaces using coking around the sampling site.*"

Comment 33

Line 434 – JP-PSCF was not used anywhere else in the paper. Did you mean TPSCF?

Response 33

The reviewer is correct. As suggested, we corrected “JP-PSCF” to “TPSCF” as follows on Line 497.

“However, CBPF and TPSCF indicated that…”

Response to Anonymous Referee #2:

General comments

This study measured TGM concentrations in South Korea and analyzed seasonal and diurnal variations of TGM. They also used the statistics analysis to correlate TGM with other pollutants and meteorological data. They tried to identify the possible TGM sources using CPF, CBPF, and TPSCF models. They found that the nearby local sources are more significant than others. Over all, this paper meets the original contributions and contains unique TGM data nearby industrial areas. The authors performed the appropriate modeling approaches to identify possible mercury sources. However, the presentation quality doesn't meet the ACP's requirement. I suggest that the paper should be carefully revised and edited prior to publication on ACP.

Comment

Response

Thank you for your comments. We carefully revised and edited that paper as suggested as is detailed in our responses to the specific comments.

Specific comments

Introduction section contains too basic and out of dated information. I suggest adding some recent mercury inventory/modeling studies in East Asia. Result and discussion contains unnecessarily much literature review. More discussions are needed. The author used statistics analysis in many places. Please provide the type of analysis in this paper.

Comment 1

Line 118 – 133: it should be combined into one paragraph.

Response 1

As suggested, the sentence was combined into one paragraph as follows on Line 125-138.

Comment 2

Line 133: So what are their results in Kim et al. 2010? What did they find?

Response 2

This meant that we got and used the Hg emissions data from the authors (Kim et al., 2010)

about iron and steel manufacturing, and a hazardous waste incinerator.

In order to clarify, we have revised the sentence as follows on Line 137 to Line 138.

*"Hg emissions **data** from iron and steel manufacturing, and a hazardous waste incinerator were estimated **based on** a previous study (Kim et al., 2010)"*

Their results in Kim et al. (2010) were described in Line 104-109.

Comment 3

Line 146-151: it doesn't fit in material & method section. Please move to results & discussion section.

Response 3

As suggested, we moved that sentence to "5. Results and Discussions" on Line 275-280 as follows.

"5.1. Meteorological data analysis

Fig. S2 shows the frequency of counts of measured wind direction occurrence by season during the sampling period. The predominant wind direction at the sampling site was W (20.9%) and WS (19.2%), and calm conditions of wind speed less than 1 m s^{-1} occurred 7.6% of the time. Compared to other seasons, however, the prevailing winds in summer were N (17.0%), NE (16.4%), S (16.4%), and SW (15.8%)."

Comment 4

Line 156-157: need to explain how often manual injections were conducted.

Response 4

Manual injections were performed prior to every field sampling campaign and we continuously operated Tekran 2537B to measure GEM concentrations in the ambient air.

In order to avoid any confusion, we have rephrased the sentence as follows on Line 159 to Line 160.

"*Manual injections were performed prior to every field sampling campaign to evaluate these automated calibrations using a saturated mercury vapor standard.*"

Comment 5

Line 164: already used CPF in Line 163. Replace "Conditional Probability Function (CPF)" with "CPF"

Response 5

As suggested, "Conditional Probability Function (CPF)" was replaced with CPF on Line 168.

Comment 6

Line 220 – 222 and line 230 – 233 are same.

Response 6

The sentence on Line 220-222 means that we computed 24hr backward trajectories starting at every hour at a height of 10, 50, and 100 m above ground level.

The sentence on Line 230-233 means that TPSCF which incorporates probability from **above different starting heights (10, 50, and 100 m above ground level)** was calculated.

In order to more clarify, we rephrased the sentence as follows on Line 236-237.

"*In this study, TPSCF which incorporates probability from above different starting heights was calculated…*"

Comment 7

Line 237: what is n_{ij} values here?

Response 7

n_{ij} is the number of trajectory segment endpoints that fall into the *ij*-th cell. This information was described in the sentence on Line 212.

In order to clarify, we added "the number of trajectory segment endpoints that fall into the *ij*-th cell" to the sentence on Line 243 as follows.

"*To minimize the effect of small* n_{ij} *(the number of trajectory segment endpoints that fall into*

the ij-th cell) values, resulting in high TPSCF values …."

Comment 8

Line 272-275: Can the author provide recent TGM data from China and other country?

Response 8

As suggested, we added recent TGM data from China and other countries in Table 1 on Line 531 and rephrased the sentence on Line 287-288.

"…and those measured in China, in Japan and other locations in Korea, however considerably lower than those measured near large Hg sources in Guangzhou, China (Table 1)."

Comment 9

Line 285 and later: if the author mentioned p-value ($p < 0.01$ or $p < 0.05$), "statistically significantly" does not have to be addressed every time. Readers already know that the author performed statistical analysis.

Response 9

After Line 285, we deleted the phrase "statistically significantly" as suggested (after Line 298).

Comment 10

Line 293: "as will be discussed later: : :." Can you indicate where and which section it was discussed?

Response 10

We have deleted the phrase "*As will be discussed later*" as follows on Line 306.

"The high TGM concentrations in fall was due to …"

Comment 11

This 5.4 section is for result and discussion. It includes too much literature review rather than discussion.

Response 11

As suggested, we rephrased the 5.4 section as following Section "*5.5. Diurnal variations*" on Line 353-426.

Comment 12

Line 346 – 348: can you explain what previous studies concluded about these diurnal variations? Needs more discussion.

Response 12

As suggested, we rephrased the sentence on Line 363-371 as follows.

"The daytime TGM concentration (5.3 ± 4.7 ng m^{-3}) was higher than that in the nighttime (4.7 ± 4.7 ng m^{-3}) ($p < 0.01$), which was similar to several previous studies (Cheng et al., 2014; Gabriel et al., 2005; Nakagawa, 1995; Stamenkovic et al., 2007) but different than another studies (Lee et al., 1998). Previous studies reported that this different is due to local sources close to the sampling site (Cheng et al., 2014; Gabriel et al., 2005), a positive correlation between TGM concentration and ambient air temperature (Nakagawa, 1995) and increased traffic (Stamenkovic et al., 2007). However, another study suggested that the higher TGM concentration during the night was due to the shallowing of the boundary layer, which concentrated the TGM near the surface (Lee et al., 1998)"

Comment 13

Line 353: "as will be discussed later…" Indicate where and which section it was discussed? What is "this" mean here? Does "this" mean lower TGM in daytime?

Response 13

In order to clarify, we have rephrased the sentence on Line 376-384 as follows.

"*Although it is possible that the land-sea breeze may affect diurnal variations in TGM concentrations since the sampling site was near the ocean and lower TGM were also observed during the daytime, the higher concentrations in the daytime than those in nighttime were due to local emission sources because the daytime temperature (14.7 ± 10.0 ºC) was statistically significantly higher than that in the nighttime (13.0 ± 9.8 ºC) (t-test, $p < 0.05$) and there was a weak but statistically significant negative correlation between TGM concentration and ambient*

air temperature (r = -0.08) (p < 0.05). In addition, there are several known Hg sources such as iron and steel manufacturing facilities including electric and sintering furnaces using coking between the sampling site and the ocean."

Comment 14

Line 355 – 356 and line 369 – 370 are same. Please rephrase or rewrite.

Response 14

As suggest, we rephrased the sentence as follows on Line 400-401.

"*TGM concentration was negatively correlated with ambient air temperature (r = -0.08)* (*p* < 0.05) *because high ambient air temperature…*"

Comment 15

Line 369 – 378: this paragraph is vague. Please clarify.

Response 15

In response to this comment, we added a following sentence as follows on Line 408-412.

"*Nonparametric correlations revealed that there is a positive correlation between TGM and ambient air temperature (r_s = 0.11, p=0.27) between 06:00-09:00. The TGM concentration was negatively correlated with O_3 (r_s = -0.33, p<0.01) but positively correlated with NO_2 (r_s = 0.21, p<0.05), suggesting that the increased traffic is the main source of TGM during these time periods.*"

Comment 16

This 5.5 section also has too much literature review rather than discussion.

Response 16

As suggested, we rephrased the Section 5.5 as follows on Line 428-474 (see the Section *5.6. CPF, CBPF and TPSCF results of TGM)*

Comment 17

Line 381 – 385: this paragraph is the result from the Section 5.4. Please move it to Section 5.4.

Response 17

As suggested, we moved the paragraph to Line 422 to Line 426.

Comment 18

Line 388 – 389: is this the only result from CPF model? Please explain the reason to adopt this model?

Response 18

We showed the CBPF result as well as CPF result. This information was described in the sentence on Line 433 to Line 436 as follows.

"…CBPF shows that the high probabilities from the west occurred under high wind speed (> 3 m s^{-1}) indicative of emissions from stacks as well as low wind speed (≤ 3 m s^{-1}) indicative of non-buoyant ground level sources (Uria-Tellaetxe and Carslaw, 2014)."

Comment 19

Line 391-393: Needs more detail explanations to clarify.

Response 19

In order to clarify, we rephrased the sentence on Line 433 to Line 436 as follows.

"CBPF shows that the high probabilities from the west occurred under high wind speed ***(> 3 m s^{-1})*** *indicative of emissions from stacks as well as low wind speed* ***(≤ 3 m s^{-1})*** *indicative of non-buoyant ground level sources (Uria-Tellaetxe and Carslaw, 2014)."*

Comment 20

Line 434: is it "TPSCF"?

Response 20

The reviewer is correct. As suggested, we corrected "JP-PSCF" to "TPSCF".

Comment 21

Line 434 – 436: the author mentioned that CPF only can provide high probabilities from the west of the site. Please delete the CPF in this sentence.

Response 21

In order to response to this comment, we rephrased the sentence as follows on Line 495-499.

"CPF only shows high probabilities to the west from the sampling site where there are large steel manufacturing facilities and waste incinerators. However, CBPF and TPSCF indicated that the dominant sources of TGM were the hazardous waste incinerators and the coastal areas in the northeast as well as the iron and manufacturing facilities in the west."

Comment 22

Line 436 – 437: same sentence as Line 412 – 413. Please rephrase or rewrite.

Response 22

As suggested, we rephrased the sentence on Line 436-437 as a following sentence on Line 499 to 500.

"The domestic passenger ships routes in the East Sea were also identified as possible source areas."

Characteristics of total gaseous mercury (TGM) concentrations in an industrial complex in southern Korea: Impacts from local sources

Yong-Seok Seo[1, 2], Seung-Pyo Jeong[1], Thomas M. Holsen[3], Young-Ji Han[4], Eunhwa Choi[5], Eun Ha Park[1], Tae Young Kim[1], Hee-Sang Eum[1], Dae Gun Park[1], Eunhye Kim[6], Soontae Kim[6], Jeong-Hun Kim[7], Jaewon Choi[8], Seung-Muk Yi[1, 2, *]

[1]Department of Environmental Health, Graduate School of Public Health, Seoul National University, 1 Gwanak, Gwanak-ro, Gwanak-gu, Seoul 151-742, South Korea

[2]Institute of Health and Environment, Seoul National University, 1 Gwanak, Gwanak-ro, Gwanak-gu, Seoul 151-742, South Korea

[3]Department of Civil and Environmental Engineering, Clarkson University, Potsdam, NY13699, USA

[4]Department of Environmental Science, Kangwon National University, 192-1, Hyoja-2-dong, Chuncheon, Kangwondo, 200-701, South Korea

[5]Asian Institute for Energy, Environment & Sustainability, Seoul National University, 1 Gwanak-ro, Gwanak-gu, Seoul 151-742, South Korea

[6]Department of Environmental, Civil and Transportation Engineering, Ajou University, Woncheon-dong, Yeongtong-gu, Suwon, 443-749, South Korea

[7]Division of Air Pollution Engineering, Department of Climate and Air Quality Research, National Institute of Environmental Research, Hwangyong-ro 42, Seogu, Incheon, 404-708, South Korea

[8]University of Pennsylvania, Philadelphia, PA19104, USA

[*]Address correspondence to Dr. Seung-Muk Yi, Graduate School of Public Health, Seoul National University, 1 Gwanak, Gwanak-ro, Gwanak-gu, Seoul 151-742, South Korea
E-mail) yiseung@snu.ac.kr
Telephone) 82-2-880-2736
Fax) 82-2-745-9104

Abstract

Total gaseous mercury (TGM) concentrations were measured every 5 min in Pohang, Gyeongsangbuk-do, Korea during summer (17 August~23 August 2012), fall (9 October~17 October 2012), winter (22 January ~29 January 2013), and spring (26 March~3 April 2013) to: 1) characterize the hourly and seasonal variations of atmospheric TGM concentrations, 2) identify the relationships between TGM and co-pollutants, and 3) identify likely source directions and locations of TGM using conditional probability function (CPF), conditional bivariate probability function (CBPF) and total potential source contribution function (TPSCF).

The TGM concentration was statistically significantly highest in fall (6.7 ± 6.4 ng m^{-3}), followed by spring (4.8 ± 4.0 ng m^{-3}), winter (4.5 ± 3.2 ng m^{-3}) and summer (3.8 ± 3.9 ng m^{-3}). There was a weak but statistically significant negative correlation between the TGM concentration and ambient air temperature *($r = -0.08$) ($p < 0.05$)*. Although the daytime temperature (14.7 ± 10.0 ºC) was statistically significantly higher than that in the nighttime (13.0 ± 9.8 ºC) ($p < 0.05$), the daytime TGM concentration (5.3 ± 4.7 ng m^{-3}) was statistically significantly higher than those in the nighttime (4.7 ± 4.7 ng m^{-3}) ($p < 0.01$), possibly due to local emissions related to industrial activities and activation of local surface emission sources. The observed ΔTGM/ΔCO was significantly lower than that of Asian long-range transport, but similar to that of local sources in Korea and in US industrial events suggesting that local sources are more important than that of long-range transport. CPF, CBPF and TPSCF indicated that the main sources of TGM were iron and manufacturing facilities, the hazardous waste incinerators and the coastal areas.

Keywords: Total gaseous mercury (TGM); co-pollutant; conditional probability function (CPF); conditional bivariate probability function (CBPF); total potential source contribution function (TPSCF)

1. Introduction

Mercury (Hg) in the atmosphere exists in three major inorganic forms including gaseous elemental mercury (GEM, Hg^0), gaseous oxidized mercury (GOM, Hg^{2+}) and particulate bound mercury (PBM, Hg(p)). GEM which is the dominant form of Hg in ambient air, (>95%) has a relatively long residence time (0.5~2 years) due to its low reactivity and solubility Schroeder and Munthe (1998). However, GOM has high water solubility and relatively strong surface adhesion properties (Han et al., 2005), so it has a short atmospheric residence time (~days). PBM is associated with airborne particles such as dust, soot, sea-salt aerosols, and ice crystals (Lu and Schroeder, 2004) and is likely produced, in part, by adsorption of GOM species such as $HgCl_2$ onto atmospheric particles (Gauchard et al., 2005; Lu and Schroeder, 2004; Sakata and Marumoto, 2005; Seo et al., 2015).

Atmospheric Hg is emitted from both natural sources (volcanoes, volatilization from aquatic and terrestrial environments) and anthropogenic sources (coal combustion, ferrous and non-ferrous metals manufacturing facilities, waste incineration and industrial boilers) (Lindberg et al., 2007; Pirrone et al., 2010; Schmeltz et al., 2011).

Atmospheric Hg released from natural and anthropogenic sources when introduced into terrestrial and aquatic ecosystem through wet and dry deposition (Mason and Sheu, 2002) can undergo various physical and chemical transformations before being deposited. Its lifetime in the atmosphere depends on its reactivity and solubility so that depending on its form it can have impacts on local, regional and global scales (Lin and Pehkonen, 1999; Lindberg et al., 2007). A portion of the Hg deposited in terrestrial environments through direct industrial discharge or atmospheric deposition is transported to aquatic system through groundwater and surface water runoff (Miller et al., 2013).

A previous study also reported that Hg directly released into terrestrial and aquatic ecosystems from industrial effluent has influenced surface water, sediment and biological tissue (Flanders et al., 2010).

Significant spatial variations in atmospheric Hg deposition near urban and industrial areas were due to local anthropogenic sources including municipal waste incinerators, medical waste incinerators, electric power generating facilities and cement kilns (Dvonch et al., 1998), ferrous and non-ferrous metal processing, iron and steel manufacturing facilities, and oil and coal combustion (Hoyer et al., 1995). Miller et al. (2013) also reported that local sources of elemental Hg are typically industrial processes including retort facilities used in the mercury mining industry to convert Hg containing minerals to elemental Hg and chlor-alkali facilities.

Annual anthropogenic Hg emissions in South Korea have been estimated to be 12.8 tons; the major anthropogenic mercury emission sources are coal combustion in thermal power plants (25.8%), oil refineries (25.5%), cement kilns (21%), incinerators (19.3%) including sludge incinerators (4.7%), municipal waste incinerators (MWIs) (3%), industrial waste incinerators (IWIs) (2.7%), hospital/medical/infectious waste incinerators (HMIWIs) (8.8%), and iron manufacturing (7%) (Kim et al., 2010).

Receptor models are often used to identify sources of air pollutants and are focused on the pollutants behavior in the ambient environment at the point of impact (Hopke, 2003). In previous studies, conditional probability function (CPF), which utilizes the local wind direction, and potential source contribution function (PSCF), which utilizes longer backward trajectories (typically 3-5 days), combined with concentration data were used to identify possible transport pathways and source locations (Hopke, 2003). While PSCF has been used

primarily to identify regional sources, it has also been used to identify local sources (Hsu et al., 2003). The objectives of this study were to characterize the hourly and seasonal variations of atmospheric TGM (the sum of the GEM and the GOM) concentrations, to identify the relationships between TGM and co-pollutant concentrations, and to identify likely source directions and locations of TGM using CPF, conditional bivariate probability function (CBPF) and total PSCF (TPSCF).

2. Materials and methods

2.1. Sampling and analysis

TGM concentrations were measured on the roof of the Korean Federation of Community Credit Cooperatives (KFCCC) building (latitude: 35.992°, longitude: 129.404°, ~10 m above ground) in Pohang city, in Gyeongsangbuk-do, a province in eastern South Korea. Gyeongsangbuk-do has a population of 2.7 million (5% of the total population and the third most populated province in South Korea) and an area of 19,030 km^2 (19% of the total area of South Korea and the largest province geographically in South Korea). Pohang city has a population of 500,000 (1% of the total population in South Korea) and an area of 605.4 km^2 (1.1% of the total area in South Korea). It is heavily industrialized with the third largest steel manufacturing facility in Asia and the fifth largest in the world. There are several iron and steel manufacturing facilities including electric and sintering furnaces using coking in Gyeongsangbuk-do including Pohang. In addition, there are several coke plants around the sampling site. The Hyungsan River divides the city into a residential area and the steel complex. Hg emissions data from iron and steel manufacturing, and a hazardous waste incinerator were estimated based on a previous study (Kim et al., 2010) (Fig. 1).

TGM concentrations were measured every 5 min during summer (17 August~23 August 2012), fall (9 October~17 October 2012), winter (22 January ~29 January 2013), and spring (26 March~3 April 2013) using a mercury vapor analyzer (Tekran 2537B) which has two gold cartridges that alternately collect and thermally desorb mercury. Ambient air at a flow rate of 1.5 L min^{-1} was transported through a 3 m-long heated sampling line (1/4" OD Teflon) in to the analyzer. The sampling line was heated at about 50 ^{o}C using heat tape to prevent water condensation in the gold traps because moisture on gold surfaces interferes with the amalgamation of Hg (Keeler and Barres, 1999). Particulate matter was removed from the sampling line by a 47 mm Teflon filter.

2.2. Meteorological data

Hourly meteorological data (air temperature, relative humidity, and wind speed and direction) were obtained from the Automatic Weather Station (AWS) operated by the Korea Meteorological Administration (KMA) (http://www.kma.go.kr) (6 km from the site). Hourly concentrations of NO_2, O_3, CO, PM_{10} and SO_2 were obtained from the National Air Quality Monitoring Network (NAQMN) (3 km from the site) (Fig. 1).

2.3. QA/QC

Automated daily calibrations were carried out for the Tekran 2537B using an internal permeation source. Two-point calibrations (zero and span) were separately performed for each gold cartridge. Manual injections were performed prior to every field sampling campaign to evaluate these automated calibrations using a saturated mercury vapor standard. The relative percent difference (RPD) between automated calibrations and manual injections was less than 2%. The recovery measured by directly injecting known amounts of four

mercury vapor standards when the sample line was connected to zero air ranged from 92 to 110% (99.4 ± 5.2% in average).

3. Model descriptions

3.1. Conditional Probability Function (CPF)

CPF was originally performed to determine which wind directions dominate during high concentration events to evaluate local source impacts (Ashbaugh et al., 1985). It has been successfully used in many previous studies (Begum et al., 2004; Kim et al., 2003a; Kim et al., 2003b; Xie and Berkowitz, 2006; Zhao et al., 2004; Zhou et al., 2004). CPF estimates the probability that the measured concentration will exceed the threshold criterion for a given wind direction. The CPF is defined as follows Eq. (1).

$$CPF_{\Delta\theta} = \frac{m_{\Delta\theta|C\geq x}}{n_{\Delta\theta}} \quad (1)$$

where, $m_{\Delta\theta}$ is the number of samples from the wind sector θ having concentration C greater than or equal to a threshold value x, and $n_{\Delta\theta}$ is the total number of samples from wind sector $\Delta\theta$. In this study, 16 sectors ($\Delta\theta = 22.5^{o}$) were used and calm winds ($\leq$ 1 m s^{-1}) were excluded from the analysis. The threshold criterion was set at above the overall average TGM concentration (5.0 ng m^{-3}). Thus, CPF indicates the potential for winds from a specific direction to contribute to high air pollution concentrations.

3.2. Conditional Bivariate Probability Function (CBPF)

CBPF couples ordinary CPF with wind speed as a third variable, allocating the measured concentration of pollutant to cells defined by ranges of wind direction and wind speed rather than to only wind direction sectors.

The CBPF is defined as follows Eq. (2).

$$CBPF_{\Delta\theta,\Delta u} = \frac{m_{\Delta\theta,\Delta u|C\geq x}}{n_{\Delta\theta,\Delta u}} \quad (2)$$

where, $m_{\Delta\theta,\Delta u}$ is the number of samples in the wind sector $\Delta\theta$ with wind speed interval Δu having concentration C greater than a threshold value x, and $n_{\Delta\theta\Delta u}$ is the total number of samples in that wind direction-speed interval. The threshold criterion was set at above the overall average TGM concentration (5.0 ng m^{-3}). The extension to the bivariate case can provide more information on the nature of the sources because different source types such as stack emission sources and ground-level sources can have different wind speed dependencies (prominent at low and high wind speed). More detailed information is described in a previous study (Uria-Tellaetxe and Carslaw, 2014).

3.3. Potential Source Contribution Function (PSCF)

The PSCF model has been extensively and successfully used in the previous studies to identify the likely source areas (Cheng et al., 1993; Han et al., 2004; Hopke et al., 2005; Lai et al., 2007; Lim et al., 2001; Poissant, 1999; Zeng and Hopke, 1989). The PSCF is a simple method that links residence time in upwind areas with high concentrations through a conditional probability field and was originally developed by Ashbaugh et al. (1985). $PSCF_{ij}$ is the conditional probability that an air parcel that passed through the ijth cell had a high concentration upon arrival at the monitoring site and is defined as the following Eq. (3).

209

210 $$PSCF_{ij} = \frac{m_{ij}}{n_{ij}} \quad (3)$$

211

212 where, n_{ij} is the number of trajectory segment endpoints that fall into the ij-th cell, and m_{ij} is the
213 number of segment endpoints in the same grid cell (ij-th cell) when the concentrations are higher
214 than a criterion value as measured at the sampling site.
215 High PSCF values in those grid cells are regarded as possible source locations. Cells including
216 emission sources can be identified with conditional probabilities close to one if trajectories that
217 have crossed the cells efficiently transport the released pollutant to the receptor site. Therefore,
218 the PSCF model provides a tool to map the source potentials of geographical areas.
219 The criterion value of PSCF for TGM concentration was set at above the overall average
220 concentration (5.0 ng m^{-3}) to identify the emission sources associated with high TGM
221 concentrations and provide a better estimation and resolution of source locations during the
222 sampling periods. The geographic area covered by the computed trajectories was divided into
223 an array of 0.05º latitude by 0.05º longitude grid cells. As will be discussed in Section 5.4, 24
224 h backward trajectories starting at every hour at a height of 10, 50, and 100 m above ground
225 level were computed using the vertical velocity model because local sources are more
226 important than that of long-range transport in this study (It should be noted that PSCF results
227 using 48 h backward trajectories had similar results as the 24 h backward trajectories). Each
228 trajectory was terminated if they exit the model top (5,000m), but advection continues along
229 the surface if trajectories intersect the ground. To generate horizontally highly resolved
230 meteorological inputs for trajectory calculations, the Weather Research and Forecast (WRF)
231 model was used to generate a coarse domain at a resolution of 27 km and a nested domain at
232 a horizontal resolution of 9 km, which geographically covers northeast Asia and the southern

part of the Korean Peninsula, respectively. The nested domain has 174 columns in the east-west direction and 114 rows in the north-south direction. PSCF was calculated with 9 km meteorological data.

In this study, TPSCF which incorporates probability from above different starting heights was calculated since backward trajectories starting at different heights traverse different distances and pathways, thus providing information that cannot be obtained from a single starting height (Cheng et al., 1993).

Generally, PSCF results show that the potential sources covered wide areas instead of indicating individual sources due to the trailing effect. The trailing effect appears since PSCF distributes a constant weight along the path of the trajectories. To minimize the effect of small n_{ij} (the number of trajectory segment endpoints that fall into the ij-th cell) values, resulting in high TPSCF values with high uncertainties, an arbitrary weight function $W(n_{ij})$ was applied to down-weight the PSCF values for the cell in which the total number of end points was less than three times the average value of the end points (Choi et al., 2011; Heo et al., 2009; Hopke et al., 1995; Polissar et al., 2001). The TPSCF value for a grid cell was defined with following Eq. (4).

$$P(TPSCF_{ij}) = \frac{P(m_{ij})_{10m} + P(m_{ij})_{50m} + P(m_{ij})_{100m}}{P(n_{ij})_{10m} + P(n_{ij})_{50m} + P(n_{ij})_{100m}} \times W \quad (4)$$

where,

253
$$W(n_{ij}) = \begin{cases} 1.0, & 3n_{ave} < n_{ij} \\ 0.8, & 2n_{ave} < n_{ij} \le 3n_{ave} \\ 0.6, & n_{ave} < n_{ij} \le 2n_{ave} \\ 0.4, & 0.5n_{ave} < n_{ij} \le n_{ave} \\ 0.2, & n_{ij} \le 0.5n_{ave} \end{cases}$$

254

255 **4. Clean Air Policy Support System (CAPSS) data**

256 In this study, the Korean National Emission Inventory estimated using Clean Air Policy
257 Support System (CAPSS) data developed by the National Institute of Environmental
258 Research (NIER) were used (http://airemiss.nier.go.kr/main.jsp (accessed December 09,
259 2015)). The CAPSS is the national emission inventory system for the air pollutants (CO,
260 NOx, SOx, TSP, PM_{10}, $PM_{2.5}$, VOCs and NH_3) which utilizes various national, regional and
261 local statistical data collected from about 150 organizations in Korea. In CAPSS, the Source
262 Classification Category (SCC) excluding fugitive dust and biomass burning based on the
263 European Environment Agency's (EEA) CORe Inventory of AIR emissions was classified
264 into the following four levels (EMEP/CORINAIR) (NIER, 2011).

265 (1) The upper level (SCC1): 11 source categories ,
266 (2) The intermediate level (SCC2): 42 source categories and
267 (3) The lower level (SCC3): 173 source categories

268

269 The sectoral contributions of emissions of South Korea, Gyeongsangbuk-do and Pohang
270 for CO, NOx, SOx, TSP, PM_{10}, $PM_{2.5}$, VOC and NH_3 are shown in Fig. S1 (See SI for
271 details).

More detailed information about SCCs in CAPSS is described in Table S1.

5. Results and Discussions

5.1. Meteorological data analysis

Fig. S2 shows the frequency of counts of measured wind direction occurrence by season during the sampling period. The predominant wind direction at the sampling site was W (20.9%) and WS (19.2%), and calm conditions of wind speed less than 1 m s^{-1} occurred 7.6% of the time. Compared to other seasons, however, the prevailing winds in summer were N (17.0%), NE (16.4%), S (16.4%), and SW (15.8%).

5.2. General characteristics of TGM

The seasonal distributions of TGM were characterized by large variability during each sampling period (Fig. 2). The average concentration of TGM during the complete sampling period was 5.0 ± 4.7 ng m^{-3} (range: 1.0-79.6 ng m^{-3}). This is significantly higher than the Northern Hemisphere background concentration (~1.5 ng m^{-3}) (Sprovieri et al., 2010) and those measured in China, in Japan and other locations in Korea, however considerably lower than those measured near large Hg sources in Guangzhou, China (Table 1). The median TGM concentration was 3.6 ng m^{-3} which was much lower than that of the average, suggesting that there were some extreme pollution episodes with very high TGM concentrations.

The TGM concentration follows a typical log-normal distribution (Fig. S3). The range of 2 to 5 ng m^{-3} dominated the distribution, accounting for more than half of the total number of samples (60.8%). The maximum frequency of 28.1% occurred between 2 and 3 ng m^{-3}. Extremely high TGM concentration events (>20 ng m^{-3}) were also observed (1.7% of the time).

296

297 *5.3. Seasonal variations*

298 The TGM concentration was statistically significantly higher in fall (6.7 ± 6.4 ng m^{-3}) ($p <$
299 0.01), followed by spring (4.8 ± 4.0 ng m^{-3}), winter (4.5 ± 3.2 ng m^{-3}) and summer (3.8 ± 3.9
300 ng m^{-3}) (Table 2). The highest concentrations (TGM > 10 ng m^{-3}) were measured more
301 frequently in fall (24.7%), and the lowest concentrations (TGM < 3 ng m^{-3}) mainly occurred
302 in summer (49.7%). The low TGM concentration in summer is likely because increased
303 mixing height (Friedli et al., 2011), and gas phase oxidation (Choi et al., 2013; Huang et al.,
304 2010; Lynam and Keeler, 2006) at higher temperatures particularly at this sampling site
305 which is close to the ocean (2 km) where oxidation involving halogens may be enhanced
306 (Holmes et al., 2009; Lin et al., 2006). The high TGM concentrations in fall was due to
307 different wind direction (see Fig. S2), sources, relationships with other pollutants and
308 meteorological conditions. More detailed information can be found in Section 5.5.
309 The average concentrations of NO_2, O_3, CO, PM_{10} and SO_2 during the complete sampling
310 period were 23.1 ± 10.8 ppbv, 24.6 ± 12.5 ppbv, 673.7 ± 487.3 ppbv, 55.5 ± 26.4 μg m^{-3} and
311 6.7 ± 4.3 ppbv, respectively. NO_2, O_3, CO, PM_{10} and SO_2 concentrations were highest in
312 spring (Table 2). There was a statistically significant positive correlation between the TGM
313 and PM_{10} (r = 0.10) ($p < 0.01$). However, the TGM concentration was not significantly
314 correlated with NO_2, CO or SO_2 concentrations, suggesting that combustion associated with
315 space heating was not a significant source of TGM (Choi et al., 2009).

316

317 *5.4. Relationship between TGM and CO*

318 CO has a significant anthropogenic source and is considered to be an indicator of
319 anthropogenic emissions (Mao et al., 2008). Previous studies reported that TGM and CO

have a strong correlation because they have similar emission sources (combustion processes) and similar long atmospheric residence times (Weiss-Penzias et al., 2003).

There was a weak positive correlation between TGM and CO in this study (r = 0.04) (p = 0.27). However there was a statistically significant correlation between TGM and CO in winter (r = 0.25) ($p < 0.05$), suggesting that TGM and CO were affected by similar, possibly distant, anthropogenic emission sources in winter.

On the other hand, there were no statistically significant correlations between TGM and CO in spring (r = 0.02) ($p = 0.78$), in summer (r = 0.13) ($p = 0.08$), or in fall (r = -0.03) ($p = 0.69$), indicating that TGM and CO were affected by different anthropogenic emission sources in these seasons.

Previous studies identified the long-range transport of mercury using the ΔTGM/ΔCO enhancement ratio (Choi et al., 2009; Jaffe et al., 2005; Kim et al., 2009; Weiss-Penzias et al., 2003; Weiss-Penzias et al., 2006). Kim et al. (2009) and Choi et al. (2009) investigated high concentration events which were defined as at least a 10 h period with hourly average TGM and CO concentrations higher than the average monthly TGM and CO concentrations. They reported that long-range transport events were characterized by high values of TGM/CO ratio (ΔTGM/ΔCO) (0.0052-0.0158 ng m^{-3} ppb^{-1}) and high correlations (r^2>0.5), whereas local events showed low ΔTGM/ΔCO (0.0005 ng m^{-3} ppb^{-1} in average) and weak correlations (r^2 < 0.5).

The observed ΔTGM/ΔCO was 0.0001 ng m^{-3} ppb^{-1} in spring, 0.0005 ng m^{-3} ppb^{-1} in summer, -0.0007 ng m^{-3} ppb^{-1} in fall, 0.0011 ng m^{-3} ppb^{-1} in winter, which are significantly lower than that indicative of Asian long-range transport (0.0046-0.0056 ng m^{-3} ppb^{-1}) (Friedli

et al., 2004; Jaffe et al., 2005; Weiss-Penzias et al., 2006), suggesting that local sources are more important than that of long-range transport in this study. The ΔTGM/ΔCO in winter (0.0011 ng m^{-3} ppb^{-1}) was similar to that of a site impacted by local sources in Korea (Kim et al., 2009) and in US industrially related events (0.0011 ng m^{-3} ppb^{-1}) (Weiss-Penzias et al., 2007).

There are also uncertainties from the potential mixing between Hg associated with long-range transported airflows and local air making it difficult to distinguish between distant and local source impacts. However, it is possible that the one-week sampling period in each season did not capture the long-range transport events, and more can be learned using a larger dataset than just using the one-week sampling period to confirm these results.

5.5. Diurnal variations

Diurnal variations of TGM (Fig. 3), co-pollutants concentrations, and meteorological data were observed (Fig. S4). TGM, O_3, CO, SO_2, and temperature in the daytime (06:00-18:00) were higher than those in the nighttime (18:00-06:00) ($p < 0.05$) except PM_{10} ($p = 0.09$) (Fig. S5). However, NO_2 during the nighttime because of relatively lower photochemical reactivity with O_3 was higher than that in daytime ($p < 0.05$) (Adame et al., 2012). TGM generally showed a consistent diurnal variation with an increase in the early morning (06:00-09:00) and a decrease in the afternoon (14:00-17:00), similar to previous studies (Dommergue et al., 2002; Friedli et al., 2011; Li et al., 2011; Liu et al., 2011; Mao et al., 2008; Shon et al., 2005; Song et al., 2009; Stamenkovic et al., 2007).

The daytime TGM concentration (5.3 ± 4.7 ng m^{-3}) was higher than that in the nighttime (4.7 ± 4.7 ng m^{-3}) ($p < 0.01$), which was similar to several previous studies (Cheng et al., 2014; Gabriel et al., 2005; Nakagawa, 1995; Stamenkovic et al., 2007) but different than

366 another studies (Lee et al., 1998). Previous studies reported that this different is due to local
367 sources close to the sampling site (Cheng et al., 2014; Gabriel et al., 2005), a positive
368 correlation between TGM concentration and ambient air temperature (Nakagawa, 1995) and
369 increased traffic (Stamenkovic et al., 2007). However, another study suggested that the higher
370 TGM concentration during the night was due to the shallowing of the boundary layer, which
371 concentrated the TGM near the surface (Lee et al., 1998).

372 In a previous study the daytime TGM concentration was relatively lower than that in the
373 nighttime because the sea breeze transported air containing low amounts of TGM from the
374 ocean during the daytime whereas the land breeze transported air containing relatively high
375 concentrations of TGM from an urban area during the nighttime (Kellerhals et al., 2003).
376 Although it is possible that the land-sea breeze may affect diurnal variations in TGM
377 concentrations since the sampling site was near the ocean and lower TGM were also observed
378 during the daytime, the higher concentrations in the daytime than those in nighttime were due
379 to local emission sources because the daytime temperature (14.7 ± 10.0 ºC) was statistically
380 significantly higher than that in the nighttime (13.0 ± 9.8 ºC) (t-test, $p < 0.05$) and there was a
381 weak but statistically significant negative correlation between TGM concentration and
382 ambient air temperature (r = -0.08) ($p < 0.05$). In addition, there are several known Hg
383 sources such as iron and steel manufacturing facilities including electric and sintering
384 furnaces using coking between the sampling site and the ocean.

385 As shown in Fig. 3 and Fig. S4, there was a weak but negative relationship between the
386 TGM concentrations and O_3 concentrations (r = -0.18) ($p < 0.01$), suggesting that oxidation
387 of GEM in the oxidizing atmosphere during periods of strong atmospheric mixing was
388 partially responsible for the diurnal variations of TGM concentrations. In addition, oxidation
389 of GEM by bromine species in the coastal area (Obrist et al., 2011) or by chloride radicals in

marine boundary layer (Laurier et al., 2003) might play a significant role. If oxidation of GEM occurred, GOM concentrations would increase. However there are uncertainties on the net effects on TGM (the sum of the GEM and the GOM) since we did not measure GOM concentrations.

Significantly different diurnal patterns have been observed at many suburban sites with the daily maximum occurring in the afternoon (12:00-15:00), possibly due to local emission sources and transport (Fu et al., 2010; Fu et al., 2008; Kuo et al., 2006; Wan et al., 2009). Other studies in Europe reported that TGM concentrations were relatively higher early in the morning or at night possibly due to mercury emissions from surface sources that accumulated in the nocturnal inversion layer (Lee et al., 1998; Schmolke et al., 1999).

TGM concentration was negatively correlated with ambient air temperature *($r = -0.08$) ($p < 0.05$)* because high ambient air temperature in the daytime will increase the height of the boundary layer and dilute the TGM, and the relatively lower boundary layer at nighttime could concentrate the TGM in the atmosphere (Li et al., 2011). Although there was a statistically significant negative correlation between the TGM concentration and ambient air temperature, there was a rapid increase in TGM concentration between 06:00-09:00 when ambient temperatures also increased possibly due to local emissions related to industrial activities, increased traffic, and activation of local surface emission sources. Similar patterns were found in previous studies (Li et al., 2011; Stamenkovic et al., 2007). Nonparametric correlations revealed that there is a positive correlation between TGM and ambient air temperature ($r_s = 0.11$, *$p=0.27$*) between 06:00-09:00. The TGM concentration was negatively correlated with O_3 ($r_s = -0.33$, *$p<0.01$*) but positively correlated with NO_2 ($r_s = 0.21$, *$p<0.05$*), suggesting that the increased traffic is the main source of TGM during these time periods.

Compared to other seasons, significantly different diurnal variations of TGM were observed in fall. The daytime TGM concentrations in fall were similar to those in other seasons, however, the nighttime TGM concentrations in fall were much higher than other seasons. As described earlier in Section 5.3, the high TGM concentrations in fall was possibly due to the relationship between other pollutants and meteorological conditions as well as different wind direction and sources. The nighttime TGM concentrations in fall were simultaneously positively correlated with PM_{10} (r=0.26) (p<0.05) and CO (r=0.21) (p<0.05) concentrations and wind speed (r=0.35) (p<0.01), suggesting that the combustion process is an important source during this period.

Based on the above results, the diurnal variations in TGM concentration are due to a combination of: 1) reactions with an oxidizing atmosphere, 2) changes in ambient temperature and 3) local emissions related to industrial activities. To supplement these conclusions CPF and CBPF were used to identify source directions and TPSCF was used to identify potential source locations.

5.6. CPF, CBPF and TPSCF results of TGM

Conventional CPF, CBPF and TPSCF plots for TGM concentrations higher than the average concentration show high source probabilities to the west in the direction of large steel manufacturing facilities and waste incinerators (Fig. 4). The CPF only shows high probabilities from the west and provides no further information, however, the CBPF shows groups of sources with the high probabilities from the west and the northeast. CBPF shows that the high probabilities from the west occurred under high wind speed (> 3 m s^{-1}) indicative of emissions from stacks as well as low wind speed (≤3 m s^{-1}) indicative of non-buoyant ground level sources (Uria-Tellaetxe and Carslaw, 2014).

As described in Section 5.4, correlations between TGM and CO revealed that TGM and CO were affected by similar anthropogenic emission sources in winter but affected by different sources in spring, summer and fall, which is supported by Fig. S6 which shows significantly different seasonal patterns of CPF and CBPF for TGM concentrations.

It is difficult to discuss about the different seasonal patterns of CPF and CBPF for TGM concentrations since there were no correlations between TGM and other pollutants in spring, summer and fall. However, compared to Fig. 4, the CPF and CBPF patterns in fall were similar to those during the whole sampling periods. Especially, the nighttime TGM concentration in fall was simultaneously positively correlated with PM_{10} ($r=0.26$) ($p<0.05$) and CO ($r=0.21$) ($p<0.05$) concentrations and wind speed ($r=0.35$) ($p<0.01$), indicating that the combustion process from the west is an important source during this period.

Since TGM showed a significant correlation with CO ($r=0.25$) ($p<0.05$) and showed a weak positive correlation with PM_{10} ($r=0.08$) ($p=0.33$) in winter, the combustion source from the west is partially responsible for this result with high wind speed.

TPSCF identified the likely sources of TGM as the iron and manufacturing facilities and the hazardous waste incinerators which are located to the west from the sampling site. A previous study reported that the waste incinerators (9%) and iron and steel manufacturing (7%) were relatively high Hg emissions sources in Korea (Kim et al., 2010). Waste incinerators emissions were due to the high Hg content in the waste (Lee et al., 2004). Emissions from iron and steel manufacturing are due to the numerous electric and sintering furnaces using coking which emits relatively high mercury concentrations (Lee et al., 2004) in Gyeongsangbuk-do including Pohang. There are several coke plants around the sampling site (http://www.poscoenc.com/upload/W/BUSINESS/PDF/ENG_PLANT_2_1_3_5.pdf (accessed December 09, 2015)). They are essential parts of the iron and steel manufacturing,

462 and the major source of atmospheric mercury related to the iron and steel manufacturing is
463 from coke production (Pacyna et al., 2006).
464 The coastal areas east of the sampling site where there are large ports were also identified
465 as the likely source areas of TGM. A previous study reported that the emissions of gaseous
466 and particulate pollutants were high during vehicular operations in port areas and from
467 marine vessel and launches (Gupta et al., 2002). Another possibility is that significant amount
468 of GEM are emitted from the ocean surface because of photo-chemically and
469 microbiologically mediated photo-reduction of dissolved GOM (Amyot et al., 1994; Zhang
470 and Lindberg, 2001). The northeast direction including the East Sea was also identified as
471 potential source areas likely because this is an area with lots of domestic passenger ships
472 routes. The south from the sampling was also identified as a likely source area of TGM where
473 Ulsan Metropolitan City, South Korea's seventh largest metropolis with a population of over
474 1.1 million is located. It includes a large petrochemical complex known as a TGM source
475 (Jen et al., 2013).
476

Conclusions

During the sampling periods, the average TGM concentration was higher than the Northern Hemisphere background concentration, however, considerably lower than those near industrial areas in China and higher than those in Japan and other locations in Korea. The median concentration of TGM was much lower than that of the average, suggesting that there were some extreme pollution episodes with very high TGM concentrations. The TGM concentration was highest in fall, followed by spring, winter and summer. The high TGM concentration in fall is due to transport from different wind directions than during the other periods. The low TGM concentration in summer is likely due to increased mixing height and gas phase oxidation at higher temperatures particularly at this sampling site which is close to the ocean (2 km) where oxidation involving halogens may be enhanced.

TGM consistently showed a diurnal variation with a maximum in the early morning (06:00-09:00) and minimum in the afternoon (14:00-17:00). Although there was a statistically significant negative correlation between the TGM concentration and ambient air temperature, the daytime TGM concentration was higher than those in the nighttime, suggesting that local emission sources are important. There was a negative relationship between the TGM concentrations and O_3 concentrations, indicating that the oxidation was partially responsible for the diurnal variations of TGM concentrations. The observed $\Delta TGM/\Delta CO$ was significantly lower than that indicative of Asian long-range transport, suggesting that local sources are more important than that of long-range transport. CPF only shows high probabilities to the west from the sampling site where there are large steel manufacturing facilities and waste incinerators. However, CBPF and TPSCF indicated that the dominant sources of TGM were the hazardous waste incinerators and the coastal areas in the northeast

as well as the iron and manufacturing facilities in the west. The domestic passenger ships routes in the East Sea were also identified as possible source areas.

Author contribution

Yong-Seok Seo conducted a design of the study, the experiments and analysis of data, wrote the initial manuscript, and finally approved the final manuscript. Seung-Pyo Jeong, Eun Ha Park, Tae Young Kim, Hee-Sang Eum, Dae Gun Park, Eunhye Kim, Jaewon Choi and Jeong-Hun Kim conducted the experiments, analysis of data, and finally approved the final manuscript. Thomas M. Holsen, Young-Ji Han and Eunhwa Choi and Soontae Kim conducted interpretation of the results, revision of the initial manuscript, and finally approved the final manuscript. Seung-Muk Yi conducted a design of the study, acquisition of data of the study, interpretation of data, and revision of the initial manuscript, and finally approved the final manuscript.

Acknowledgments

We thank National Institute of Environmental Research (NIER) for providing CAPSS data. This work was supported by Brain Korea 21 (BK21) Plus Project (Center for Healthy Environment Education and Research) through the National Research Foundation (NRF) of Korea and Korea Ministry of Environment (MOE) as “the Environmental Health Action Program”.

521 **Table List**

525

526 **Figure List**

532 **Table 1.** Comparison with previous studies for TGM concentrations.

Country	Location	Sampling period	TGM conc. (ng m^{-3})	Classifications	Reference
China	Mt. Waliguan, Qinghai–Tibet Plateau	Oct. 2007 ~ Sep. 2009	2.1	Remote	Fu et al. (2015)
China	Mt. Hengduan, Qinghai–Tibet Plateau	Jul. 2010 ~ Oct. 2010	2.5	Remote	Fu et al. (2015)
China	Nanjing, Jiangsu	Jan. 2011 ~ Oct. 2011	7.9	Urban	Hall et al. (2014)
China	Mt. Dinghu, Guangdong	Oct. 2009 ~ Apr. 2010	5.1	Rural	Chen et al. (2013)
China	Guangzhou, Guangdong	Nov. 2010 ~ Nov. 2011	4.6	Urban	Chen et al. (2013)
China	Nanjing, Jiangsu	Jan. 2011 ~ Dec. 2011	7.9	Urban	Zhu et al. (2012)
China	Guangzhou, Guangdong	Jul. 1999 ~ Jul. 2000	13.5 - 25.4	Urban	Fang et al. (2004)
China	Gui Yang, Guizhou	Jan. 2010 ~ Feb. 2010	8.4	Urban	Feng et al. (2004)
China	Changchun, Jilin	Sep. 1999 ~ Aug. 2000	9.1-15.4	Suburban	Fang et al. (2004)
Japan	Fukuoka	Jun. 2012 ~ May 2013	2.33	Urban	(Marumoto et al., 2015)
Japan	Tokai-mura	Oct. 2005 ~ Aug. 2006	3.8	Suburban	Osawa et al. (2007)
Japan	Tokyo	Apr. 2000 ~ Mar. 2001	2.7	Urban	Sakata and Marumoto (2002)
Korea	Seoul	1987 ~ 2013	3.7	Urban	Kim et al. (2016)
Korea	Gangwon-do, Chuncheon	2006 ~ 2009	2.1	Rural	Han et al. (2014)
Korea	Seoul	Feb. 2005 ~ Feb. 2006	3.2	Urban	Kim et al. (2009)
Korea	Seoul	Feb. 2005 ~ Dec. 2006	3.4	Urban	Choi et al. (2009)
Korea	Seoul	19 Sep. 1997 ~ 29 Sep. 1997 27 May. 1998 ~ 18 Jun. 1998	3.6	Urban	Kim and Kim (2001)
Korea	Gyeongsangbuk-do, Pohang	17 Aug. 2012 ~ 23 Aug. 2012 9 Oct. 2012 ~ 17 Oct. 2012 22 Jan. 2013 ~ 29 Jan. 2013 26 Mar. 2013 ~ 3 Apr. 2013	5.0	Urban	This study

533

534 **Table 2.** Summary of atmospheric concentrations of TGM and co-pollutants, and meteorological data. Note that TGM was measured every 5-
535 min, and other pollutants and meteorological data were measured every 1-hour.

		TGM (ng m^{-3})	NO_2 (ppb)	O_3 (ppb)	CO (ppb)	PM_{10} (μg m^{-3})	SO_2 (ppb)	Temperature (℃)	Wind speed (m s^{-1})	Humidity (%)	Solar radiation (MJ m^{-2})
Spring	**N**	2139	189	215	215	215	215	216	216	216	216
	Average	4.8 ± 4.0	25.3 ± 9.0	29.4 ± 14.2	766.5 ± 505.2	70.1 ± 26.0	7.6 ± 3.8	10.5 ± 4.2	2.2 ± 1.2	56.2 ± 16.8	0.82 ± 1.09
	Range	1.9 – 45.3	8 – 55	2 – 58	300 – 3100	28 - 204	5 - 35	1.1 – 21.6	0.4 – 6.2	19.0 – 94.0	0 – 3.44
Summer	**N**	1863	187	188	187	188	188	186	180	186	141
	Average	3.8 ± 3.9	18.3 ± 9.2	18.9 ± 10.1	697.3 ± 689.7	35.1 ± 15.8	6.5 ± 6.2	26.6 ± 4.2	2.2 ± 1.1	82.5 ± 13.9	0.40 ± 0.69
	Range	1.2 – 75.9	4 – 44	5 – 48	200 – 3300	12 – 87	2 - 27	19.7 – 34.1	0.1 – 6.4	43 - 98	0 – 2.92
Fall	**N**	2226	212	212	212	212	211	216	216	216	216
	Average	6.7 ± 6.4	25.0 ± 7.8	23.7 ± 13.1	662.7 ± 350.2	58.1 ± 17.8	5.3 ± 3.5	17.4 ± 3.2	2.1 ± 0.8	54.5 ± 14.7	0.62 ± 0.90
	Range	1.0 – 79.6	9 – 53	6 – 69	300 – 2900	20 - 145	3 - 39	11.7 – 25.2	0.5 – 4.5	12 - 79	0 – 2.90
Winter	**N**	1917	188	187	188	188	186	192	192	192	192
	Average	4.5 ± 3.2	23.5 ± 14.7	26.1 ± 8.7	556.4 ± 298.9	56.3 ± 30.5	7.4 ± 2.5	1.1 ± 4.3	2.8 ± 1.1	46.3 ± 24.5	0.43 ± 0.71
	Range	1.3 – 66.4	5 – 74	1 – 41	200 – 2400	18 – 161	5 – 24	-0.65 – 10.1	0.5 – 6.0	11 - 90	0 – 2.34
Total	**N**	8145	776	802	802	803	800	810	804	810	765
	Average	5.0 ± 4.7	23.1 ± 10.8	24.6 ± 12.5	673.7 ± 487.3	55.5 ± 26.4	6.7 ± 4.3	13.8 ± 9.9	2.3 ± 1.1	59.4 ± 22.1	0.59 ± 0.90
	Range	1.0 – 79.6	4 – 74	1 – 69	200 – 3300	12 – 204	2 – 39	-6.5 – 34.1	0.1 – 6.4	11 - 98	0 – 3.44

536

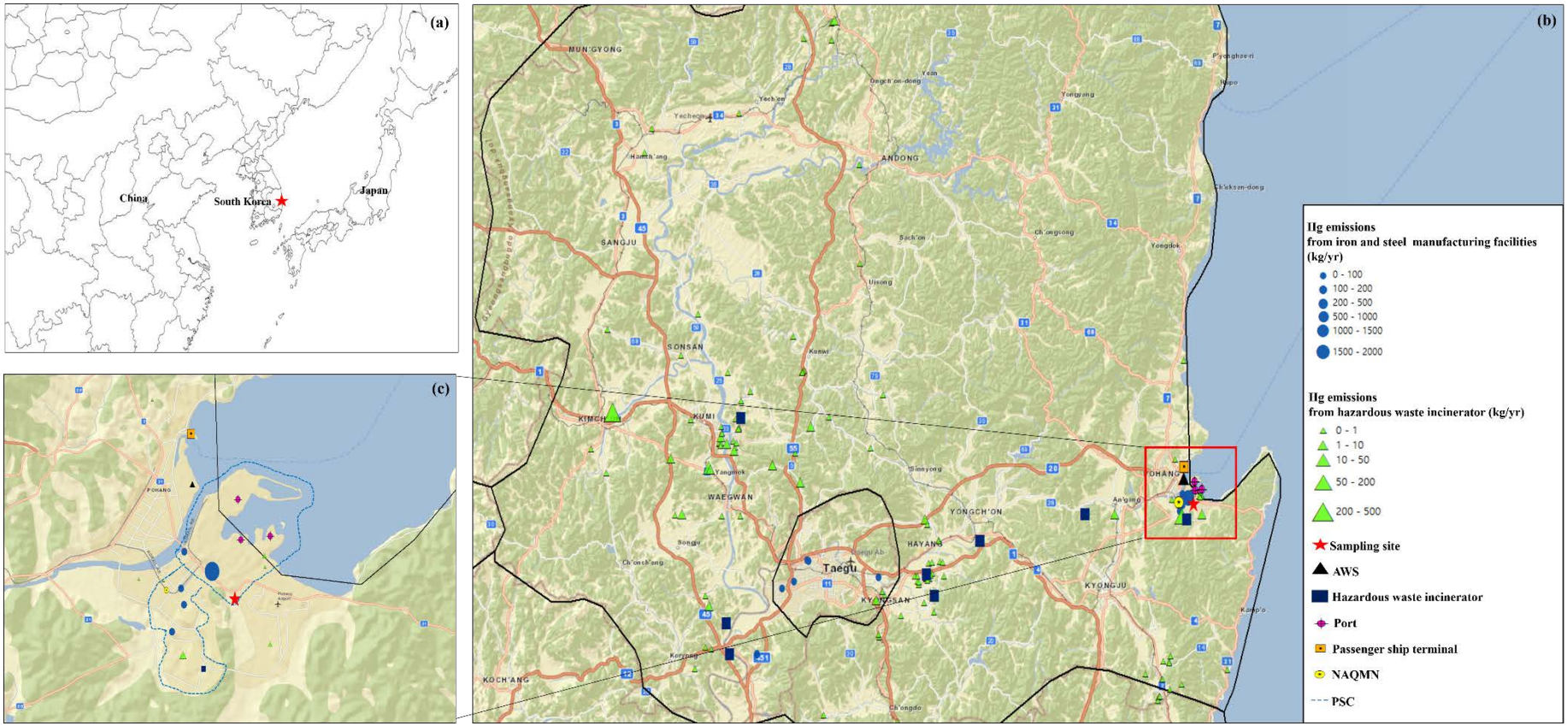

537

Fig. 1. The location of sampling site in this study ((a) South Korea, (b) Gyeongsangbuk-do and (c) Pohang). AWS, NAQMN and PSC represent Automatic Weather Station, National Air Quality Monitoring Network and Pohang Steel Complex, respectively.

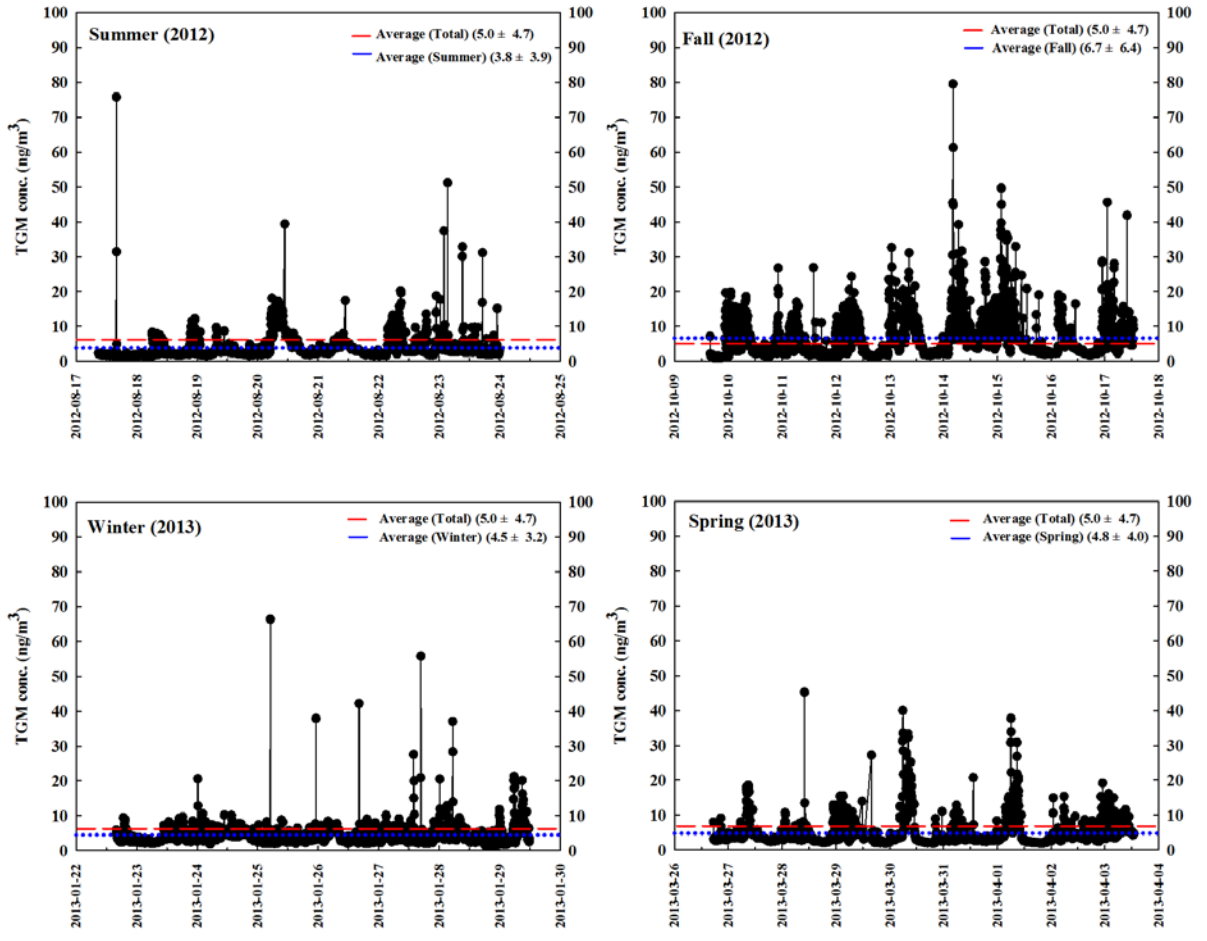

538

539 **Fig. 2.** Time-series of TGM concentrations in this study.

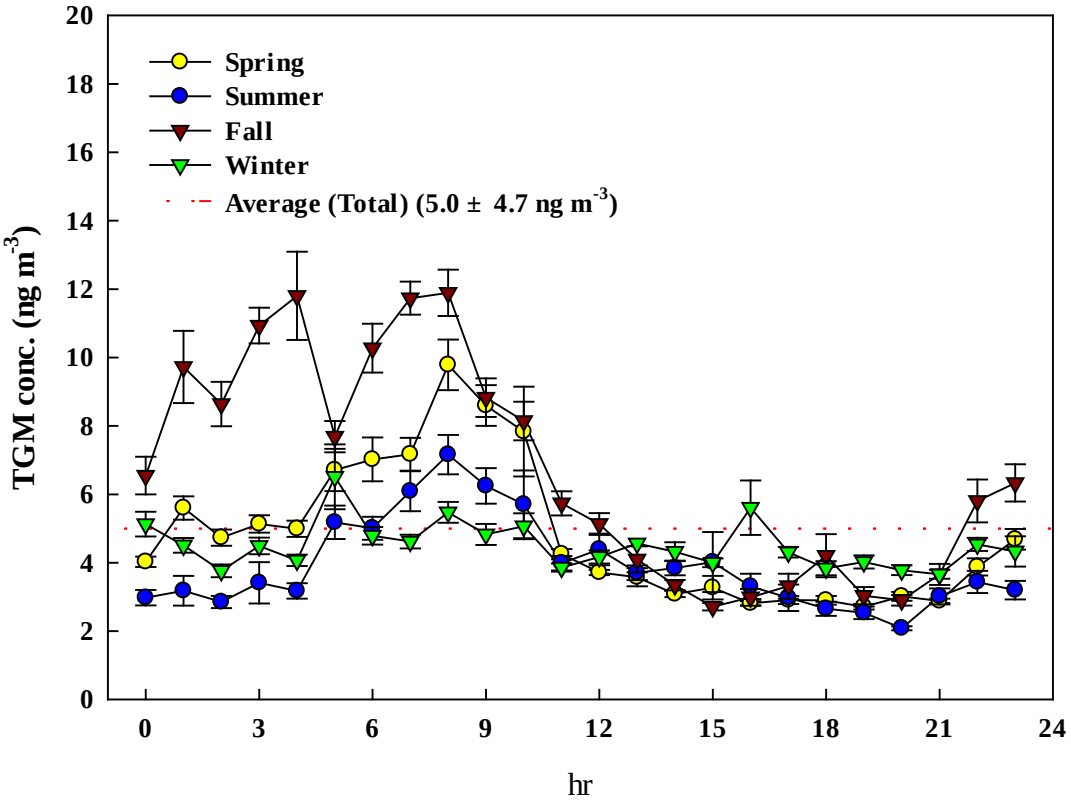

Fig. 3. The diurnal variations of TGM concentrations during the sampling periods. The error bars represent standard error.

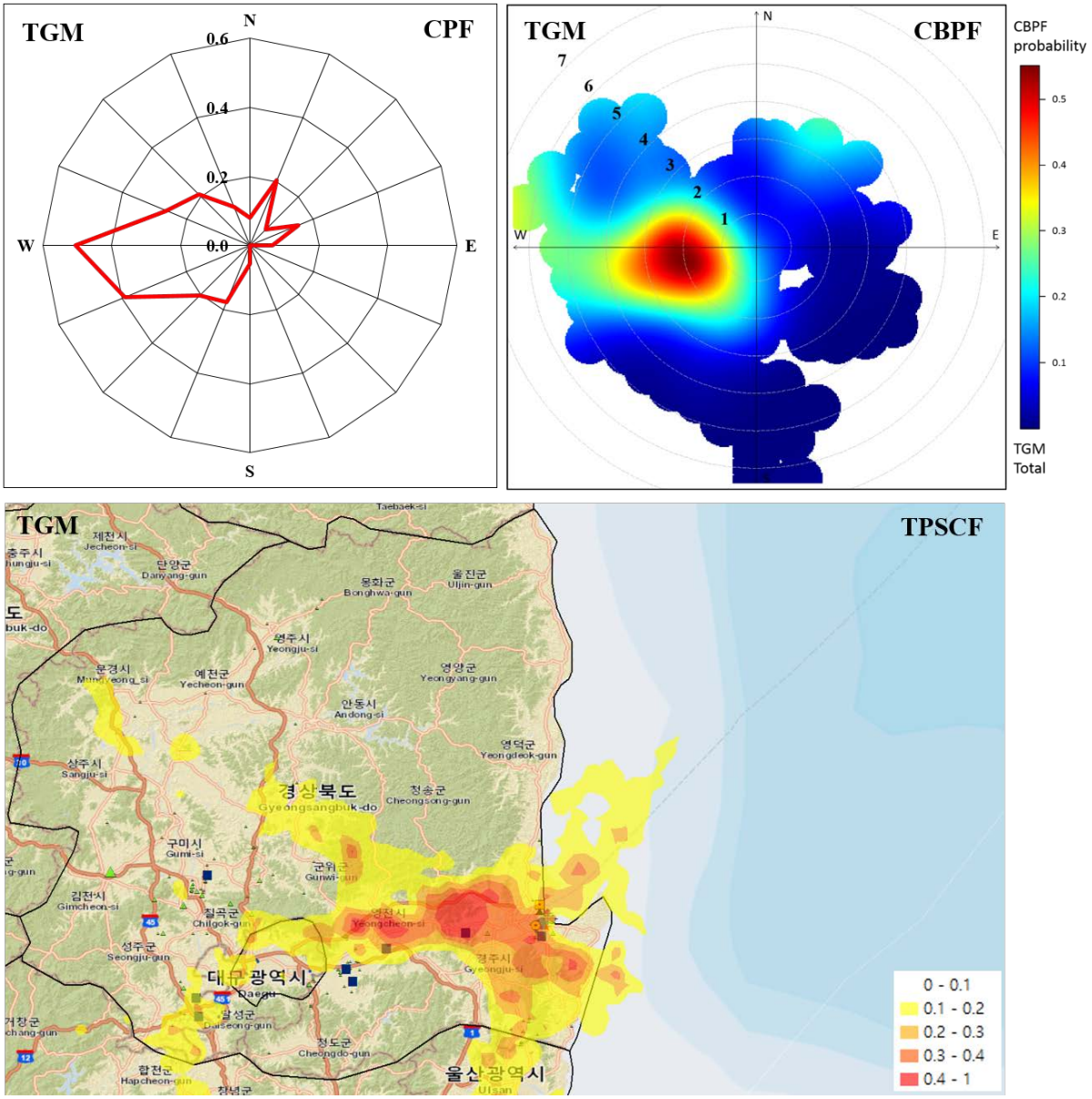

Fig. 4. CPF, CBPF and TPSCF plots for TGM higher than average concentration. The radial axes of CPF and CBPF are the probability and the wind speed (m s^{-1}), respectively.

References

Adame, J., Notario, A., Villanueva, F., and Albaladejo, J.: Application of cluster analysis to surface ozone, NO_2 and SO_2 daily patterns in an industrial area in Central-Southern Spain measured with a DOAS system, Sci. Total Environ., 429**,** 281-291, 2012.

Amyot, M., Mcqueen, D. J., Mierle, G., and Lean, D. R.: Sunlight-induced formation of dissolved gaseous mercury in lake waters, Environ. Sci. Technol., 28**,** 2366-2371, 1994.

Ashbaugh, L. L., Malm, W. C., and Sadeh, W. Z.: A residence time probability analysis of sulfur concentrations at Grand Canyon National Park, Atmospheric Environment (1967), 19**,** 1263-1270, 1985.

Begum, B. A., Kim, E., Biswas, S. K., and Hopke, P. K.: Investigation of sources of atmospheric aerosol at urban and semi-urban areas in Bangladesh, Atmos. Environ., 38**,** 3025-3038, 2004.

Chen, L., Liu, M., Xu, Z., Fan, R., Tao, J., Chen, D., Zhang, D., Xie, D., and Sun, J.: Variation trends and influencing factors of total gaseous mercury in the Pearl River Delta—A highly industrialised region in South China influenced by seasonal monsoons, Atmos. Environ., 77**,** 757-766, 2013.

Cheng, I., Zhang, L., Mao, H., Blanchard, P., Tordon, R., and Dalziel, J.: Seasonal and diurnal patterns of speciated atmospheric mercury at a coastal-rural and a coastal-urban site, Atmos. Environ., 82**,** 193-205, 2014.

Cheng, M. D., Hopke, P. K., and Zeng, Y.: A receptor-oriented methodology for determining source regions of particulate sulfate observed at Dorset, Ontario, Journal of Geophysical Research: Atmospheres (1984–2012), 98**,** 16839-16849, 1993.

Choi, E.-M., Kim, S.-H., Holsen, T. M., and Yi, S.-M.: Total gaseous concentrations in mercury in Seoul, Korea: local sources compared to long-range transport from China and Japan, Environ. Pollut., 157**,** 816-822, 2009.

Choi, E., Heo, J.-B., Hopke, P. K., Jin, B.-B., and Yi, S.-M.: Identification, apportionment, and photochemical reactivity of non-methane hydrocarbon sources in Busan, Korea, Water, Air, Soil Pollut., 215**,** 67-82, 2011.

Choi, H.-D., Huang, J., Mondal, S., and Holsen, T. M.: Variation in concentrations of three mercury (Hg) forms at a rural and a suburban site in New York State, Sci. Total Environ., 448**,** 96-106, 2013.

Dommergue, A., Ferrari, C. P., Planchon, F. A., and Boutron, C. F.: Influence of anthropogenic sources on total gaseous mercury variability in Grenoble suburban air (France), Sci. Total Environ., 297**,** 203-213, 2002.

Dvonch, J., Graney, J., Marsik, F., Keeler, G., and Stevens, R.: An investigation of source–receptor relationships for mercury in south Florida using event precipitation data, Sci. Total Environ., 213**,** 95-108, 1998.

Fang, F., Wang, Q., and Li, J.: Urban environmental mercury in Changchun, a metropolitan city in Northeastern China: source, cycle, and fate, Sci. Total Environ., 330**,** 159-170, 2004.

Feng, X., Shang, L., Wang, S., Tang, S., and Zheng, W.: Temporal variation of total gaseous mercury in the air of Guiyang, China, Journal of Geophysical Research: Atmospheres (1984–2012), 109, 2004.

Flanders, J., Turner, R., Morrison, T., Jensen, R., Pizzuto, J., Skalak, K., and Stahl, R.: Distribution, behavior, and transport of inorganic and methylmercury in a high gradient stream, Appl. Geochem., 25**,** 1756-1769, 2010.

595 Friedli, H., Arellano Jr, A., Geng, F., Cai, C., and Pan, L.: Measurements of atmospheric
596 mercury in Shanghai during September 2009, Atmos. Chem. Phys., 11**,** 3781-3788,
597 2011.
598 Friedli, H. R., Radke, L. F., Prescott, R., Li, P., Woo, J. H., and Carmichael, G. R.: Mercury
599 in the atmosphere around Japan, Korea, and China as observed during the 2001 ACE-
600 Asia field campaign: Measurements, distributions, sources, and implications, Journal
601 of Geophysical Research: Atmospheres (1984–2012), 109, 2004.
602 Fu, X., Feng, X., Dong, Z., Yin, R., Wang, J., Yang, Z., and Zhang, H.: Atmospheric gaseous
603 elemental mercury (GEM) concentrations and mercury depositions at a high-altitude
604 mountain peak in south China, Atmos. Chem. Phys., 10**,** 2425-2437, 2010.
605 Fu, X., Feng, X., Zhu, W., Wang, S., and Lu, J.: Total gaseous mercury concentrations in
606 ambient air in the eastern slope of Mt. Gongga, South-Eastern fringe of the Tibetan
607 plateau, China, Atmos. Environ., 42**,** 970-979, 2008.
608 Fu, X., Zhang, H., Lin, C.-J., Feng, X., Zhou, L., and Fang, S.: Correlation slopes of
609 GEM/CO, GEM/CO 2, and GEM/CH 4 and estimated mercury emissions in China,
610 South Asia, the Indochinese Peninsula, and Central Asia derived from observations in
611 northwestern and southwestern China, Atmospheric Chemistry and Physics, 15**,** 1013-
612 1028, 2015.
613 Gabriel, M. C., Williamson, D. G., Brooks, S., and Lindberg, S.: Atmospheric speciation of
614 mercury in two contrasting Southeastern US airsheds, Atmos. Environ., 39**,** 4947-
615 4958, 2005.
616 Gauchard, P.-A., Ferrari, C. P., Dommergue, A., Poissant, L., Pilote, M., Guehenneux, G.,
617 Boutron, C. F., and Baussand, P.: Atmospheric particle evolution during a nighttime
618 atmospheric mercury depletion event in sub-Arctic at Kuujjuarapik/Whapmagoostui,
619 Quebec, Canada, Sci. Total Environ., 336**,** 215-224, 2005.
620 Gupta, A., Patil, R., and Gupta, S.: Emissions of gaseous and particulate pollutants in a port
621 and harbour region in India, Environ. Monit. Assess., 80**,** 187-205, 2002.
622 Hall, C. B., Mao, H., Ye, Z., Talbot, R., Ding, A., Zhang, Y., Zhu, J., Wang, T., Lin, C.-J.,
623 and Fu, C.: Sources and Dynamic Processes Controlling Background and Peak
624 Concentrations of TGM in Nanjing, China, Atmosphere, 5**,** 124-155, 2014.
625 Han, Y.-J., Holsen, T. M., Hopke, P. K., Cheong, J.-P., Kim, H., and Yi, S.-M.: Identification
626 of source locations for atmospheric dry deposition of heavy metals during yellow-
627 sand events in Seoul, Korea in 1998 using hybrid receptor models, Atmos. Environ.,
628 38**,** 5353-5361, 2004.
629 Han, Y.-J., Holsen, T. M., Hopke, P. K., and Yi, S.-M.: Comparison between back-trajectory
630 based modeling and Lagrangian backward dispersion modeling for locating sources of
631 reactive gaseous mercury, Environ. Sci. Technol., 39**,** 1715-1723, 2005.
632 Han, Y.-J., Kim, J.-E., Kim, P.-R., Kim, W.-J., Yi, S.-M., Seo, Y.-S., and Kim, S.-H.:
633 General trends of atmospheric mercury concentrations in urban and rural areas in
634 Korea and characteristics of high-concentration events, Atmos. Environ., 94**,** 754-764,
635 2014.
636 Heo, J.-B., Hopke, P., and Yi, S.-M.: Source apportionment of $PM_{2.5}$ in Seoul, Korea, Atmos.
637 Chem. Phys., 9**,** 4957-4971, 2009.
638 Holmes, C. D., Jacob, D. J., Mason, R. P., and Jaffe, D. A.: Sources and deposition of
639 reactive gaseous mercury in the marine atmosphere, Atmos. Environ., 43**,** 2278-2285,
640 2009.
641 Hopke, P., Barrie, L., Li, S. M., Cheng, M. D., Li, C., and Xie, Y.: Possible sources and
642 preferred pathways for biogenic and non-sea-salt sulfur for the high Arctic, Journal of
643 Geophysical Research: Atmospheres (1984–2012), 100**,** 16595-16603, 1995.

644 Hopke, P. K.: Recent developments in receptor modeling, J. Chemometrics, 17**,** 255-265,
645 2003.
646 Hopke, P. K., Zhou, L., and Poirot, R. L.: Reconciling trajectory ensemble receptor model
647 results with emissions, Environ. Sci. Technol., 39**,** 7980-7983, 2005.
648 Hoyer, M., Burke, J., and Keeler, G. 1995. Atmospheric sources, transport and deposition of
649 mercury in Michigan: two years of event precipitation. *Mercury as a Global*
650 *Pollutant.* Springer.
651 Hsu, Y.-K., Holsen, T. M., and Hopke, P. K.: Comparison of hybrid receptor models to locate
652 PCB sources in Chicago, Atmos. Environ., 37**,** 545-562, 2003.
653 Huang, J., Choi, H.-D., Hopke, P. K., and Holsen, T. M.: Ambient mercury sources in
654 Rochester, NY: results from principle components analysis (PCA) of mercury
655 monitoring network data, Environ. Sci. Technol., 44**,** 8441-8445, 2010.
656 Jaffe, D., Prestbo, E., Swartzendruber, P., Weiss-Penzias, P., Kato, S., Takami, A.,
657 Hatakeyama, S., and Kajii, Y.: Export of atmospheric mercury from Asia, Atmos.
658 Environ., 39**,** 3029-3038, 2005.
659 Jen, Y.-H., Yuan, C.-S., Hung, C.-H., Ie, I.-R., and Tsai, C.-M.: Tempospatial variation and
660 partition of atmospheric mercury during wet and dry seasons at sensitivity sites within
661 a heavily polluted industrial city, Aerosol Air Qual. Res, 13**,** 13-23, 2013.
662 Keeler, G., and Barres, J.: Sampling and Analysis for Atmospheric Mercury, Center for
663 Environmental Research Information, Cincinati, 1999.
664 Kellerhals, M., Beauchamp, S., Belzer, W., Blanchard, P., Froude, F., Harvey, B., Mcdonald,
665 K., Pilote, M., Poissant, L., and Puckett, K.: Temporal and spatial variability of total
666 gaseous mercury in Canada: results from the Canadian Atmospheric Mercury
667 Measurement Network (CAMNet), Atmos. Environ., 37**,** 1003-1011, 2003.
668 Kim, E., Hopke, P. K., and Edgerton, E. S.: Source identification of Atlanta aerosol by
669 positive matrix factorization, J. Air Waste Manage. Assoc., 53**,** 731-739, 2003a.
670 Kim, E., Larson, T. V., Hopke, P. K., Slaughter, C., Sheppard, L. E., and Claiborn, C.: Source
671 identification of $PM_{2.5}$ in an arid Northwest US City by positive matrix factorization,
672 Atmospheric Research, 66**,** 291-305, 2003b.
673 Kim, J.-H., Park, J.-M., Lee, S.-B., Pudasainee, D., and Seo, Y.-C.: Anthropogenic mercury
674 emission inventory with emission factors and total emission in Korea, Atmos.
675 Environ., 44**,** 2714-2721, 2010.
676 Kim, K.-H., Brown, R. J., Kwon, E., Kim, I.-S., and Sohn, J.-R.: Atmospheric mercury at an
677 urban station in Korea across three decades, Atmos. Environ., 131**,** 124-132, 2016.
678 Kim, K.-H., and Kim, M.-Y.: Some insights into short-term variability of total gaseous
679 mercury in urban air, Atmos. Environ., 35**,** 49-59, 2001.
680 Kim, S.-H., Han, Y.-J., Holsen, T. M., and Yi, S.-M.: Characteristics of atmospheric
681 speciated mercury concentrations (TGM, Hg (II) and Hg (p)) in Seoul, Korea, Atmos.
682 Environ., 43**,** 3267-3274, 2009.
683 Kuo, T.-H., Chang, C.-F., Urba, A., and Kvietkus, K.: Atmospheric gaseous mercury in
684 Northern Taiwan, Sci. Total Environ., 368**,** 10-18, 2006.
685 Lai, S.-O., Holsen, T. M., Hopke, P. K., and Liu, P.: Wet deposition of mercury at a New
686 York state rural site: concentrations, fluxes, and source areas, Atmos. Environ., 41**,**
687 4337-4348, 2007.
688 Laurier, F. J., Mason, R. P., Whalin, L., and Kato, S.: Reactive gaseous mercury formation in
689 the North Pacific Ocean's marine boundary layer: A potential role of halogen
690 chemistry, Journal of Geophysical Research: Atmospheres (1984–2012), 108, 2003.
691 Lee, D. S., Dollard, G. J., and Pepler, S.: Gas-phase mercury in the atmosphere of the United
692 Kingdom, Atmos. Environ., 32**,** 855-864, 1998.

693 Lee, S. J., Seo, Y.-C., Jurng, J., Hong, J.-H., Park, J.-W., Hyun, J. E., and Lee, T. G.:
694 Mercury emissions from selected stationary combustion sources in Korea, Sci. Total
695 Environ., 325**,** 155-161, 2004.
696 Li, Z., Xia, C., Wang, X., Xiang, Y., and Xie, Z.: Total gaseous mercury in Pearl River Delta
697 region, China during 2008 winter period, Atmos. Environ., 45**,** 834-838, 2011.
698 Lim, C.-J., Cheng, M.-D., and Schroeder, W. H.: Transport patterns and potential sources of
699 total gaseous mercury measured in Canadian high Arctic in 1995, Atmos. Environ.,
700 35**,** 1141-1154, 2001.
701 Lin, C.-J., and Pehkonen, S. O.: The chemistry of atmospheric mercury: a review, Atmos.
702 Environ., 33**,** 2067-2079, 1999.
703 Lin, C.-J., Pongprueksa, P., Lindberg, S. E., Pehkonen, S. O., Byun, D., and Jang, C.:
704 Scientific uncertainties in atmospheric mercury models I: Model science evaluation,
705 Atmos. Environ., 40**,** 2911-2928, 2006.
706 Lindberg, S., Bullock, R., Ebinghaus, R., Engstrom, D., Feng, X., Fitzgerald, W., Pirrone, N.,
707 Prestbo, E., and Seigneur, C.: A synthesis of progress and uncertainties in attributing
708 the sources of mercury in deposition, AMBIO: A Journal of the Human Environment,
709 36**,** 19-33, 2007.
710 Liu, N., Qiu, G., Landis, M. S., Feng, X., Fu, X., and Shang, L.: Atmospheric mercury
711 species measured in Guiyang, Guizhou province, southwest China, Atmospheric
712 Research, 100**,** 93-102, 2011.
713 Lu, J. Y., and Schroeder, W. H.: Annual time-series of total filterable atmospheric mercury
714 concentrations in the Arctic, Tellus B, 56**,** 213-222, 2004.
715 Lynam, M. M., and Keeler, G. J.: Source–receptor relationships for atmospheric mercury in
716 urban Detroit, Michigan, Atmos. Environ., 40**,** 3144-3155, 2006.
717 Mao, H., Talbot, R., Sigler, J., Sive, B., and Hegarty, J.: Seasonal and diurnal variations of
718 Hg over New England, Atmospheric Chemistry and Physics, 8**,** 1403-1421, 2008.
719 Marumoto, K., Hayashi, M., and Takami, A.: Atmospheric mercury concentrations at two
720 sites in the Kyushu Islands, Japan, and evidence of long-range transport from East
721 Asia, Atmos. Environ., 117**,** 147-155, 2015.
722 Mason, R. P., and Sheu, G. R.: Role of the ocean in the global mercury cycle, Global
723 biogeochemical cycles, 16**,** 40-1-40-14, 2002.
724 Miller, C. L., Watson, D. B., Lester, B. P., Lowe, K. A., Pierce, E. M., and Liang, L.:
725 Characterization of soils from an industrial complex contaminated with elemental
726 mercury, Environ. Res., 125**,** 20-29, 2013.
727 Nakagawa, R.: Studies on the levels in atmospheric concentrations of mercury in Japan,
728 Chemosphere, 31**,** 2669-2676, 1995.
729 Nier: National Air Pollutants Emission 2011 (in Korean), 2011.
730 Obrist, D., Tas, E., Peleg, M., Matveev, V., Faïn, X., Asaf, D., and Luria, M.: Bromine-
731 induced oxidation of mercury in the mid-latitude atmosphere, Nature Geoscience, 4**,**
732 22-26, 2011.
733 Osawa, T., Ueno, T., and Fu, F.: Sequential variation of atmospheric mercury in Tokai-mura,
734 seaside area of eastern central Japan, Journal of Geophysical Research: Atmospheres
735 (1984–2012), 112, 2007.
736 Pacyna, E. G., Pacyna, J. M., Steenhuisen, F., and Wilson, S.: Global anthropogenic mercury
737 emission inventory for 2000, Atmos. Environ., 40**,** 4048-4063, 2006.
738 Pirrone, N., Cinnirella, S., Feng, X., Finkelman, R., Friedli, H., Leaner, J., Mason, R.,
739 Mukherjee, A., Stracher, G., and Streets, D.: Global mercury emissions to the
740 atmosphere from anthropogenic and natural sources, Atmospheric Chemistry and
741 Physics, 10**,** 5951-5964, 2010.

742 Poissant, L.: Potential sources of atmospheric total gaseous mercury in the St. Lawrence
743 River valley, Atmos. Environ., 33**,** 2537-2547, 1999.
744 Polissar, A. V., Hopke, P. K., and Harris, J. M.: Source regions for atmospheric aerosol
745 measured at Barrow, Alaska, Environ. Sci. Technol., 35**,** 4214-4226, 2001.
746 Sakata, M., and Marumoto, K.: Formation of atmospheric particulate mercury in the Tokyo
747 metropolitan area, Atmos. Environ., 36**,** 239-246, 2002.
748 Sakata, M., and Marumoto, K.: Wet and dry deposition fluxes of mercury in Japan, Atmos.
749 Environ., 39**,** 3139-3146, 2005.
750 Schmeltz, D., Evers, D. C., Driscoll, C. T., Artz, R., Cohen, M., Gay, D., Haeuber, R.,
751 Krabbenhoft, D. P., Mason, R., and Morris, K.: MercNet: a national monitoring
752 network to assess responses to changing mercury emissions in the United States,
753 Ecotoxicology, 20**,** 1713-1725, 2011.
754 Schmolke, S. R., Schroeder, W., Kock, H., Schneeberger, D., Munthe, J., and Ebinghaus, R.:
755 Simultaneous measurements of total gaseous mercury at four sites on a 800km
756 transect: spatial distribution and short-time variability of total gaseous mercury over
757 central Europe, Atmos. Environ., 33**,** 1725-1733, 1999.
758 Schroeder, W. H., and Munthe, J.: Atmospheric mercury—an overview, Atmos. Environ., 32**,**
759 809-822, 1998.
760 Seo, Y.-S., Han, Y.-J., Holsen, T. M., Choi, E., Zoh, K.-D., and Yi, S.-M.: Source
761 identification of total mercury (TM) wet deposition using a Lagrangian particle
762 dispersion model (LPDM), Atmos. Environ., 104**,** 102-111, 2015.
763 Shon, Z.-H., Kim, K.-H., Kim, M.-Y., and Lee, M.: Modeling study of reactive gaseous
764 mercury in the urban air, Atmos. Environ., 39**,** 749-761, 2005.
765 Song, X., Cheng, I., and Lu, J.: Annual atmospheric mercury species in downtown Toronto,
766 Canada, J. Environ. Monit., 11**,** 660-669, 2009.
767 Sprovieri, F., Pirrone, N., Ebinghaus, R., Kock, H., and Dommergue, A.: A review of
768 worldwide atmospheric mercury measurements, Atmospheric Chemistry and Physics,
769 10**,** 8245-8265, 2010.
770 Stamenkovic, J., Lyman, S., and Gustin, M. S.: Seasonal and diel variation of atmospheric
771 mercury concentrations in the Reno (Nevada, USA) airshed, Atmos. Environ., 41**,**
772 6662-6672, 2007.
773 Uria-Tellaetxe, I., and Carslaw, D. C.: Conditional bivariate probability function for source
774 identification, Environ. Model. Software, 59**,** 1-9, 2014.
775 Wan, Q., Feng, X., Lu, J., Zheng, W., Song, X., Han, S., and Xu, H.: Atmospheric mercury in
776 Changbai Mountain area, northeastern China I. The seasonal distribution pattern of
777 total gaseous mercury and its potential sources, Environ. Res., 109**,** 201-206, 2009.
778 Weiss-Penzias, P., Jaffe, D., Swartzendruber, P., Hafner, W., Chand, D., and Prestbo, E.:
779 Quantifying Asian and biomass burning sources of mercury using the Hg/CO ratio in
780 pollution plumes observed at the Mount Bachelor Observatory, Atmos. Environ., 41**,**
781 4366-4379, 2007.
782 Weiss-Penzias, P., Jaffe, D. A., Mcclintick, A., Prestbo, E. M., and Landis, M. S.: Gaseous
783 elemental mercury in the marine boundary layer: Evidence for rapid removal in
784 anthropogenic pollution, Environ. Sci. Technol., 37**,** 3755-3763, 2003.
785 Weiss-Penzias, P., Jaffe, D. A., Swartzendruber, P., Dennison, J. B., Chand, D., Hafner, W.,
786 and Prestbo, E.: Observations of Asian air pollution in the free troposphere at Mount
787 Bachelor Observatory during the spring of 2004, Journal of Geophysical Research:
788 Atmospheres (1984–2012), 111, 2006.

789 Xie, Y., and Berkowitz, C. M.: The use of positive matrix factorization with conditional
790 probability functions in air quality studies: an application to hydrocarbon emissions in
791 Houston, Texas, Atmos. Environ., 40**,** 3070-3091, 2006.
792 Zeng, Y., and Hopke, P.: A study of the sources of acid precipitation in Ontario, Canada,
793 Atmospheric Environment (1967), 23**,** 1499-1509, 1989.
794 Zhang, H., and Lindberg, S. E.: Sunlight and iron (III)-induced photochemical production of
795 dissolved gaseous mercury in freshwater, Environ. Sci. Technol., 35**,** 928-935, 2001.
796 Zhao, W., Hopke, P. K., and Karl, T.: Source identification of volatile organic compounds in
797 Houston, Texas, Environ. Sci. Technol., 38**,** 1338-1347, 2004.
798 Zhou, L., Kim, E., Hopke, P. K., Stanier, C. O., and Pandis, S.: Advanced factor analysis on
799 Pittsburgh particle size-distribution data special issue of aerosol science and
800 technology on findings from the Fine Particulate Matter Supersites Program, Aerosol
801 Science and Technology, 38**,** 118-132, 2004.
802 Zhu, J., Wang, T., Talbot, R., Mao, H., Hall, C., Yang, X., Fu, C., Zhuang, B., Li, S., and
803 Han, Y.: Characteristics of atmospheric total gaseous mercury (TGM) observed in
804 urban Nanjing, China, Atmospheric Chemistry and Physics, 12**,** 12103-12118, 2012.